Cancer stem cell marker DCLK1 reprograms small extracellular vesicles toward migratory phenotype in gastric cancer cells

Annalisa L.E. Carli[1,2], Shoukat Afshar-Sterle[1,2,*], Alin Rai[3,4,*], Haoyun Fang[3], Ryan O'Keefe[1,2], Janson Tse[1,2], Fleur M. Ferguson[6,7], Nathanael S. Gray[6,7], Matthias Ernst[1,2], David W. Greening[3,4,5,8,#], Michael Buchert[1,2,#]

[1] Cancer Inflammation Laboratory, Olivia Newton-John Cancer Research Institute, Heidelberg, VIC, Australia
[2] School of Cancer Medicine, La Trobe University, Bundoora, VIC, Australia
[3] Baker Heart and Diabetes Institute, Molecular Proteomics, Melbourne, VIC, Australia
[4] Central Clinical School, Monash University, Melbourne, VIC, Australia
[5] Department of Biochemistry and Genetics, La Trobe Institute for Molecular Science, La Trobe University, Melbourne, VIC, Australia.
[6] Department of Cancer Biology, Dana-Farber Cancer Institute, Boston, MA 02215, USA
[7] Department of Biological Chemistry and Molecular Pharmacology, Harvard Medical School, Boston, MA 02115, USA
[8] Baker Department of Cardiometabolic Health, University of Melbourne, Melbourne, VIC, Australia
* These authors contributed equally to this work

 # Address for correspondence
Michael Buchert, PhD
Tumour Microenvironment and Cancer Signaling Group
Olivia Newton-John Cancer Research Institute
145 Studley Road, Heidelberg VIC 3084 Australia
Email: Michael.Buchert@onjcri.org.au

David W. Greening, Ph D
Molecular Proteomics Group
Baker Heart and Diabetes Institute
75 Commercial Road, Melbourne VIC 3004 Australia
Email: David.Greening@baker.edu.au

Keywords
DCLK1, Extracellular vesicles, Gastric cancer, Cell migration, Proteome.

Abstract

Doublecortin-like kinase 1 (DCLK1) is a putative cancer stem cell marker, a promising diagnostic and prognostic maker for malignant tumors and a proposed driver gene for gastric cancer (GC). DCLK1 overexpression in a majority of solid cancers correlates with lymph node metastases, advanced disease and overall poor-prognosis. In cancer cells, DCLK1 expression has been shown to promote epithelial-to-mesenchymal transition (EMT), driving disruption of cell-cell adhesion, cell migration and invasion. Here, we report that DCLK1 influences small extracellular vesicle (sEV/exosome) biogenesis in a kinase-dependent manner. sEVs isolated from DCLK1 overexpressing human GC cell line MKN1 ($MKN1^{OE}$-sEVs), promote the migration of parental (non-transfected) MKN1 cells ($MKN1^{PAR}$). Quantitative proteome analysis of $MKN1^{OE}$-sEVs revealed enrichment in migratory and adhesion regulators (STRAP, CORO1B, BCAM, COL3A, CCN1) in comparison to $MKN1^{PAR}$-sEVs. Moreover, using DCLK1-IN-1, a specific small molecule inhibitor of DCLK1, we reversed the increase in sEV size and concentration in contrast to other EV subtypes, as well as kinase-dependent cargo selection of proteins involved in EV biogenesis (KTN1, CHMP1A, MYO1G) and migration and adhesion processes (STRAP, CCN1). Our findings highlight a specific role of DCLK1-kinase dependent cargo selection for sEVs and shed new light on its role as a regulator of signaling in gastric tumorigenesis.

Statement of significance of the study

Gastric cancer (GC) is the 3rd leading cause of cancer mortality worldwide, responsible for over 800,000 deaths in 2018 and ranks 5th for cancer incidence. The importance of understanding the formation and development of GC is crucial to developing early detection tools and better therapeutic treatments. Although *DCLK1* gene amplification, overexpression and somatic missense mutations are frequently observed in human GC, the mechanisms by which DCLK1 contributes to gastric tumorigenesis remains poorly understood. Here we show that DCLK1 expression in the GC cell line MKN1 impacts small extracellular vesicle (sEV) biogenesis both quantitatively and qualitatively in a kinase-dependent manner, revealing a hitherto unknown role for this putative oncogenic kinase. By combining functional and protein dissection of human GC cell-derived sEVs, we show a DCKL1-dependent regulation of sEVs. These findings will enable future studies seeking to characterize the underlying signaling of cancer stem cells and have implications in defining and therapeutically targeting specific pro-tumorigenic signaling drivers, including kinases such as DCKL1.

Introduction

Doublecortin-like kinase 1 (DCLK1) was first described in 1999 as a close homologue of doublecortin (DCX) protein, encoded by a gene associated with brain development and neuronal migration.[1–3] In the last decade, DCLK1 emerged as a marker of cancer stem cells (CSC) and tumor-initiating cells in the GI tract.[4–6] However, more recent reports also imply a direct functional role of DCLK1 in promoting an epithelial-to-mesenchymal transition (EMT) in cancer cells and a pluripotent/stem cell state under both homeostatic and pathological conditions.[7–25] In 2013, a comprehensive genomic and molecular analysis of 100 primary gastric tumors identified DCLK1 as novel potential driver of GC.[26] A strong correlation between DCLK1 expression and low overall survival was presented in a recent meta-analysis, and correlations between DCLK1 and anti-tumor immune responses and stromal components within the tumor micro-environment (TME) was found in gastric and colorectal cancers.[27,28] We hypothesized whether the altered immune responses and stromal components in these DCLK1 high GI-tumors might be an indirect result of the microtubule associated function of DCLK1 resulting in altered intercellular communication.

DCLK1 and DCX are microtubule-associated protein (MAP) family members, regulating the dynamic turnover and distribution of microtubules. Microtubules are involved in a range of essential cellular processes like cellular shape, polarity, migration, cell division, and kinesin driven vesicle and organelle transport.[29,30] DCLK1 and DCX share no homology to other MAPs, and binds to microtubules via their two in tandem doublecortin domains (DCs). [31,32] Unlike classical MAPs, which bind along the ridges of the microtubule protofilament, DCLK1 binds in the valleys between the protofilaments. Resulting in stabilized microtubules without overlapping kinesin motor protein binding sites.[33–37] In addition, the DC domains bind to both polymerized and unpolymerized α/β-tubulin facilitating the polymerization process at the microtubule plus-ends.[38] In contrast to DCX, DCLK1 contains a functional serine/threonine kinase domain at the C-terminal tail which negatively regulates microtubule-binding affinity of DCLK1 through auto-phosphorylation of the DC domains.[39] Whilst DCX stimulates microtubule polymerization *in vitro*, purified full-length DCLK1 does not, unless the protein is in the presence of a phosphatase or its kinase domain is rendered non-functional by inactivating point mutations or specific kinase inhibitors.[39] This suggests that the kinase domain of DCLK1 is a negative regulator of microtubule polymerization and stabilization, at least *in vitro*. In addition, within neurons DCLK1 supports kinesin-3 mediated cargo transport to dendrites and involvement in synaptic vesicle trafficking.[40–45] Suggesting that DCLK1 might be directly involved in vesicular trafficking and as a result indirectly influences intercellular communication.

The cellular secretome represents a fundamental means of intercellular communication. This complex mixture of proteins, lipids and nucleic acids allows for the regulation of a broad range of cellular behaviors and physiological functions. Changes in the abundance of components of the secretome are observed in many diseases, including cancer and actively shape the TME to contribute to tumor progression[46–54]. Extracellular vesicles (EVs) are secreted lipid-encapsulated vesicles representing an active element of the cell secretome.[55] EVs include plasma membrane–derived large EVs (termed microvesicles, 100-1,500 nm size)[56–59], endosomal-derived small EVs (termed exosomes, 30-200 nm size)[58–61], midbody remnants (200-600 nm)[62,63] and exomeres (~30 nm size)[64,65] , all are well-established mediators of cancer pathology.[66–68] Even though exosomes

and microvesicles have different biological origin, their sizes and biomarkers overlap,[58,59,69–72] as such we used the consensus MISEV guidelines to term these EVs as either large or small EVs.[68] Over the last decade, cancer derived EVs have been established as multifaceted paracrine and autocrine regulators of the TME[73] affecting both cancer and non-cancer cells (i.e., immune and stromal cells[74–77]) alike. Creating a milieu conducive to cancer cell survival, proliferation, evasion of immune surveillance and to migration, invasion and the spread of cancer cells to local lymph nodes and distant sites.[73,78–85] DCLK1 is a GI CSC marker and sEVs secreted by CSCs have attracted a particular interest due to their potential use as regenerative mediators and targets for clinical anti-cancer therapies. Isolated renal CSC-sEVs were able to render recipient cells resistant to cytotoxic drugs and induced the formation of a pre-metastatic niche in vivo.[86] Another study showed that CSC-sEVs reprogrammed cells in the TME towards a pro-angiogenic and pro-metastatic phenotype.[87] Recently, it has been shown that cancer-derived sEVs induce epigenetic changes in stem cells, influencing their function in the TME.[88] These reports support a role for sEVs tumor initiation, promotion and progression. Therefore, we hypothesized that DCLK1 could drive critical pathology in GC mediated by sEVs. Here, we present a specific role of DCLK1-kinase dependent cargo selection for sEVs and shed new light on its role as a regulator of signaling in gastric tumorigenesis.

Materials and methods

Cell culture

The human GC cell lines MKN1 and MKN28 were obtained from JCRB Cell Bank. The human GC cell line AGS was obtained from the ATCC. MKN1, MKN28 and AGS were cultured in RPMI-1640 + GlutaMax (Gibco), supplemented with 10% (v/v) fetal calf serum (FCS) (Moregate biotech). Telomerase-immortalized human foreskin fibroblasts (BJ-hTERT) were kindly provided by Rick Pearson (Peter MacCallum Cancer Centre) and cultured in DMEM (Gibco™) + 20 mM HEPES, 17% (v/v) Medium 199 (Gibco™), 15% (v/v) FCS, and 1% (v/v) GlutaMAX™ L-alanyl-L-glutamine dipeptide (Gibco™).Cells were maintained at 37 °C with 10% CO_2.

The *DCLK1* isoform 1 (accession NM_004734) was PCR amplified from plasmid RC217050 (Origene) using forward primer 5' agc aag ctt gcc acc atg tcc ttc ggc aga gac atg gag 3'and reverse primer 5' acg gga tcc cta cat cct ggt tgc gtc ttc gtc 3' and subcloned into pcDNA3 using HindIII and BamHI restriction sites. The construct was verified by Sanger sequencing and transfected into MKN1 using lipofectamine 2000 (Invitrogen). Cells were selected for 4 weeks in culture medium supplemented with with 0.4 mg/mL Genetecin. DCLK1 protein expression was validated by western blot. Cells were imaged with inverted microscope (Zeiss Axio observer 5) and Zen-blue imaging software.

DCLK1-IN-1 dose-response assessment

To avoid confounding results caused by potential cytotoxicity of the DCLK1-IN-1 small molecule inhibitor, we performed a dose-response assessment in order to select a concentration of DCLK1-IN-1 that was well below the IC_{50}. For the dose-response assessment 7.5×10^3 $MKN1^{PAR}$ and $MKN1^{OE}$ cells were seeded in 96-well plate (Gibco) in quadruplicates, and subjected to a concentration range [0.003, 0.01, 0.03, 0.1, 0.3, 1, 3, 10, 30, 100 µM] of DCLK1-IN-1 small molecule inhibitor or DMSO control.[89,90] After 72 hrs, cell toxicity was quantified using MTS-reagent (Promega) and absorbance was measured at 490 nm. The IC_{50} values were determined of the Log_{10} transformed

concentrations (X) with a non-linear regression curve fit ($Y = Bottom + \frac{Top-Bottom}{1+\frac{X}{IC50}}$) using GraphPad Prism (v.8.4.3).

EV collection, purification and preparation

For the MKN1 cells, one week prior to EV collection, the FCS in the cell culture media was changed to 10% (v/v) EV depleted FCS, FCS was centrifuged at 100,000 x g for 18 hrs to remove EVs.[91] For EV collection 8×10^6 cells were seeded in a 5-layer T-1000 flask (Millipore), in 200 mL RPMI-1640 + GlutaMax, supplemented with 10% (v/v) EV-depleted FCS. Cells were cultured for 48 hrs prior to collection of conditioned media (CM) in the presence of either 1 µM DCLK1-IN-1 ($MKN1^{OE+INH}$) or DMSO control ($MKN1^{PAR}$/$MKN1^{OE}$). Five independent replicates of each $MKN1^{PAR}$, $MKN1^{OE}$, and $MKN1^{OE+INH}$ CM (5 x 200 mL) were subjected to differential ultracentrifugation as previously described[91,92] (**Figure 1C**). In brief, the CM was centrifuged (Rotina 380R) at 500 x *g* for 5 min 4 °C to remove dead cells, the supernatant subsequently centrifuged (Rotina 380R) at 2000 x *g* for 10 min 4 °C to remove cell debris. Of the supernatant 180 mL was aliquoted in to 6 fractions, each 30 mL and centrifuged at 10,000 x *g* for 30 minutes at 4 °C (SW 28, Beckman Coulter, Optima L-90k Ultracentrifuge). Supernatant was transferred to new tube and centrifuged at 100,000 x *g* for 60 min at 4 °C (SW 32Ti, Beckman Coulter, Optima L-90k Ultracentrifuge). The 10,000 x *g* (10k) pellets contain large EVs (lEVs), while the 100,000 x *g* (100k) pellets contain sEVs. To remove any co-isolated or bound factors, the 10k and 100k pellets were washed in 100 µL PBS (Gibco), pooled per condition per replicate (n=5), and centrifuged at either 10,000 x *g* for 30 min at 4 °C (Eppendorf Centrifuge 5430R) or 100,000 x *g* for 60 min at 4 °C (TLA 55, Beckman Coulter, Optima MAX-TL Ultracentrifuge), respectively. The pooled lEVs (10k) and sEV (100k) pellets were resuspended in 50 µL PBS and aliquoted for immediate use or stored at -80 °C for further downstream use.

Nanoparticle tracking analysis

Vesicle size was determined using NanoSight NS300, Nanoparticle tracking analysis (NTA) (Malvern) fitted with a NS300 flow-cell top plate with a 405 nm laser. lEV and sEV samples (1 µg/µL) in filtered (0.2 µm) Milli-Q (1:1,000 dilution) were injected with 1 mL syringes (BD) (detection threshold = 10, flowrate = 50, temperature = 25 ºC). For each sample, 5 replicate 60 s video captures were made. To calculate vesicle size and concentration, videos were analysed as described using NTA software 3.0 (ATA Scientific). [93]

Protein lysate preparation and Western blot analysis

sEVs and lEVs were lysed in sodium dodecyl sulphate (SDS) 2% (v/v), 50 mM triethylammonium bicarbonate (TEAB), pH 8.0, ultrasonicated (10 min) and centrifuged at 16,000*g* for 10 min at 4 °C, and quantified by microBCA (Life Technologies). sEV and lEV relative protein abundance was normalized to their corresponding MKN^{PAR} sEVs or lEVs of the same collection date. SDS-PAGE (Invitrogen) was performed (200 V, 35 min) on denatured (70 °C, 10 min) protein lysate (15 µg, 50 mM Dithiothreitol (DTT), 125 mM Tris–HCl, pH 6.8, 12.5 % (v/v) glycerol, 0.02 % (w/v) bromophenol blue). Proteins were transferred to PVDF-membranes using iBLOT system (Invitrogen). Membranes were blocked in blocking-buffer (5 % (w/v) milk in PBS-0.1 % Tween-20) for 1 hr at RT and subsequently probed with primary antibodies (1:1000 dilution in blocking buffer) over night at 4 °C against ALIX (Cell Signaling Technology, #2172), TSG-101 (BD Biosciences, #612696), DCLK1 (Abnova,

#H00009201-A01), and GAPDH (Sigma-Aldrich, #G9545). Membranes were subsequently incubated with secondary HRP-linked antibodies goat anti-mouse (DAKO, #P0447, 1:7500) or goat anti-rabbit (DAKO, #P0448, 1:7500) for 1 hr at RT with orbital shaking. Protein bands were visualized using ECL-substrate (Pierce) and Chemidoc™ (Biorad XRS, imagelab™ software).

Transwell cell migration assay

EV-depleted FCS was used for all transwell migration assays to fully attribute the effects upon cell migration to the added EVs and not bovine derived EVs present within FCS.[91] Transwell migration assays were performed using 8 µm transwell inserts (Falcon) seeded with 4 x 10^4 $MKN1^{PAR}$ cells in 100 µL serum-free RPMI-1640 + Glutamax (Gibco). Cells were supplemented with either 30 µg/mL $MKN1^{PAR}$-, $MKN1^{OE}$-, or $MKN1^{OE+INH}$-derived sEVs or lEVs, or vehicle (PBS). Inserts were nested onto 24-well plate (Falcon), as chemoattractant 20% (v/v) EV-depleted FCS was added to RPMI-1640 + Glutamax and incubated for 48 hrs (37 °C). For co-culture migration assays, 2 x 10^5 $MKN1^{PAR}$ or $MKN1^{OE}$ cells were seeded in a 24-well plate (falcon) (bottom chamber), 24h after seeding media was replaced with 500 µL 10% (v/v) EV-depleted FCS in RPMI 1640 and cells were cultured for 48h. 4-8 x 10^4 MKN1, MKN28, AGS or BJ1-hTERT cells were seeded in 300 µL serum-free media in 8 µm transwell inserts (Falcon) (top chamber) and co-cultured for 72h. For transwell migration and co-culture migration assays all non-migrating cells were removed with cotton-swabs and inserts were dual fixed with 4% (v/v) paraformaldehyde in PBS for 10 minutes at RT and 10 minutes with ice cold methanol (100%). Cells were stained using Diff-Quik staining solution (Millipore). Washed and air-dried membranes were cut out prior to mounting onto glass slide with dibutyl phthalate polystyrene xylene (DPX, Sigma). Slides were scanned and analyzed using Aperio ImageScope and eSlide Manager (Leica Biosystems).

Proteomic liquid chromatography–tandem mass spectrometry

For mass spectrometry-based proteomics[91], lysed samples (10 µg) were normalized and reduced with 10 mM DTT for 45 min at 50 °C followed by alkylation with 10 mM iodoacetamide for 30 min at 25 °C in the dark. The reaction was quenched to a final concentration of 20 mM DTT. Lysates were precipitated with six volumes of acetone overnight at -20 °C. Protein pellets were centrifuged at 10,000 x *g*, 10 min at 4 °C and resuspended in 50 mM TEAB, pH 8.0. Samples digested with trypsin (Promega, V5111) at a 1:50 enzyme-to-substrate ratio for 16 h at 37 °C. The peptide mixture was acidified to a final concentration of 2% formic acid, 0.1% trifluoroacetic acid (TFA) and centrifuged at 16,000*g* for 5 min, frozen at -20 °C for 30 min, and dried by vacuum centrifugation. For proteomic analysis, peptides were resuspended in 2% acetonitrile, 0.07% TFA, quantified by Fluorometric Peptide Assay and normalized to 1 µg per 3 µL.

Peptides were analyzed on a Dionex UltiMate NCS-3500RS nanoUHPLC coupled to a Q-Exactive HF-X hybrid quadrupole-Orbitrap mass spectrometer equipped with a nanospray ion source in positive mode as described.[94] Peptides were loaded (Acclaim PepMap100 C18 5 µm beads with 100 Å pore-size, Thermo Fisher Scientific) and separated (1.9-µm particle size C18, 0.075 × 250 mm, Nikkyo Technos Co. Ltd) with a gradient of 2–28% acetonitrile containing 0.1% formic acid over 110 minutes at 300 nL min^{-1} at 55°C. An MS1 scan was acquired from 350–1,650 m/z (60,000 resolution, 3 × 10^6 automatic gain control (AGC), 128 mseconds injection time) followed by MS/MS data-dependent acquisition (top 25) with collision-induced dissociation and detection in the ion trap (30,000 resolution, 1 ×10^5 AGC, 60 mseconds injection time, 28% normalized collision energy, 1.3 m/z

quadrupole isolation width). Unassigned precursor ions charge states and slightly charged species were rejected and peptide match disabled. Selected sequenced ions were dynamically excluded for 30 seconds.

Data Processing and Bioinformatics Pipeline

Peptide identification and quantification were performed as described previously using MaxQuant (v1.6.14) with its built-in search engine Andromeda.[62,94–97] Tandem mass spectra were searched against Homo sapiens (human) reference proteome (74,811 entries, downloaded 1-2020) supplemented with common contaminants. Search parameters included carbamidomethylated cysteine as fixed modification and oxidation of methionine and N-terminal protein acetylation as variable modifications. Data was processed using trypsin/P as the proteolytic enzyme with up to 2 missed cleavage sites allowed. The search tolerance and fragment ion mass tolerance were set to 7 ppm and 0.5 Da, respectively, at less than 1% false discovery rate on peptide spectrum match (PSM) level employing a target-decoy approach at peptide and protein levels. Label free quantification (LFQ) algorithm in MaxQuant was used to obtain quantification intensity values and processed using Perseus as described.[74] LFQ intensities were Log2 transformed after removing contaminants and reverse identifications. Proteins with no missing values among all sample groups are subjected to two-tail t-test with p-value adjusted at 5% permutation-based FDR. Missing values between technical replicates imputed using Perseus built-in imputation feature from a normal distribution with 1.8 downshift and 0.3 width. Normalized intensities were Log2 transformed, with statistical analyses performed using Student's T-test or ANOVA (q-value <0.05 was considered significant). Gene enrichment functional annotation clustering analysis was performed using DAVID and Reactome pathway bioinformatics recourses.[98] Graphpad Prism and Rstudio were used for visualization of analysis.

Results

DCLK1 overexpression increases cell protrusions and secretion of small extracellular vesicles (sEVs).

In light of the frequent overexpression of DCLK1 in solid tumors and its associated role as a cancer stem cell marker and putative driver of GC,[5,17,21,26,28,99–101] we established a clonal $MKN1^{OE}$ GC cell line, which stably overexpressed DCLK1 at a level approximately 4.5 fold higher compared to parental MKN1 ($MKN1^{PAR}$) cells (**Figure S1A**). Consistent with the reported role of DCLK1 as an inducer of EMT in various cancer cells,[13,19–23] DCLK1 overexressing MKN1 cells ($MKN1^{OE}$) display morphologically different to $MKN1^{PAR}$ cells (**Figure 1A**). While the $MKN1^{PAR}$ GC cells already have a mesenchymal-like morphology, upon DCLK1 overexpression we observe an increased number of cellular protrusions suggesting increased plasma membrane dynamics in $MKN1^{OE}$ cells (**Figure 1A**). In light of the increased membrane dynamics observed in cells overexpressing DCLK1 and the pivotal role that membrane forces play in the shedding of extracellular vesicles, we investigated the impact of DCLK1 and of its catalytic kinase activity on the release and composition of EVs. Consistent with previous reports on colorectal and pancreatic cancer cells, DCLK1-IN-1 had little effect on cell viability at concentrations up to 1 µM with an IC_{50} of 14 and 49 µM for $MKN1^{PAR}$ and $MKN1^{OE}$ cells, respectively (**Figure 1B**). Based on these results and the known IC_{50} of 57 nM for the inhibition of the

catalytic activity of the DCLK1 kinase, [89] we decided to use DCLK1-IN-1 at a concentration of 1 µM for all treatments in this study.

We collected conditioned media from MKN1^{PAR} cells and MKN1^{OE} cells grown for 48 hr in presence or absence of DCLK1-IN-1 and subsequently purified sEVs using differential ultracentrifugation to separate small EVs from large EVs (**Figure 1C**). Bio-marker expression of sEVs (containing exosomes) was confirmed for endomsomal-derived TSG101 and ALIX, revealing separation/enrichment of sEVs from lEVs and total cell lysate; however, we did not detect DCLK1 in either lEVs or sEVs (**Figures 1D, S1B-D**).The relative EV protein abundance was significantly increased in MKN1^{OE}-sEVs and MKN1^{OE+INH}-lEVs (**Figures 1E, S1E**). Interestingly, when DCLK1 is overexpressed there is a significant increase in total particles/mL (AUC) as well as the concentration of "larger" MKN1^{OE}-(s/l)EVs (200-600 nm), both observations are reversed upon DCLK1-inhibition (**Figures 1F, S1F-G**). Collectively, DCLK1 overexpression induces cellular protrusions and increases the amount of enlarged vesicles released, the latter is reversed upon DCLK1 inhibition.

Quality control of sEV proteome replicates

Endosomal-derived EVs traffic along microtubules to the plasma membrane as part of multivesicular endosomes (MVEs) as intraluminal vesicles[55,102–104], in contrast to EVs originating from the plasma membrane. The endosomal EVs are smaller (30-200 nm) than plasma membrane EVs (100-1,500 nm) and therefore more likely to end up in the sEV fraction. In addition, the lEV fraction consists of a heterogeneous pool of EVs (different exosome types, microvesicles)[62,71] and had approximately 2.5 Log_2 fold lower yield (AUC) (**Figure S1G**), hence only the composition of sEVs was analysed by mass spectrometry.

To investigate the capacity of DCLK1 in regulating sEV proteome composition, we performed quantitative proteomics on MKN1^{PAR}, MKN1^{OE}, and MKN1^{OE+INH} sEVs. Proteomics analysis identified 1492 unique proteins with high stringency (present in 4 or more replicates) across all sample groups, with 1290, 1265, and 1362 proteins in each group, respectively (**Figure S2A, Table S1**). Proteomics analysis further identified and validated comparable abundance of EV marker proteins, ALIX, TSG101, CD81, CD82, FLOT1 and FLOT2 (**Figure S2B, Table S1)**. To assess data variance and sample grouping, we performed a correlation matrix (**Figure S2C**) and principal component analysis (**Figure S2D**), demonstrating that MKN1^{OE} and MKN1^{OE+INH} sEV proteomes clustered together and could be distinguished from MKN1^{PAR} sEVs. This revealed that our replicate MKN1^{OE4} (OE4) consistently generated outlier results and therefore was excluded from further downstream analyses (**Figures S2C-D**).

Overexpression of DCLK1 induces reprogramming of sEV composition to support cell adhesion and cell migration *in vitro.*

To investigate the influence of DCLK1 overexpression on sEV proteomes, we initially compared sEV proteomes between MKN1^{OE} and MKN1^{PAR} cells, and observed significantly (students t-test p<0.05) altered abundance of 381 of the identified 1424 proteins, including 96 down- and 283 up-regulated (**Figure 2A, Table S2-3**). We next performed enrichment map analysis of these proteins to gain insight into enriched pathways and functions (Gene Ontology (GO), KEGGs). Subsequent gene

enrichment analysis revealed that a third of these proteins are assigned to either cell adhesion (gene ontology GO: 0007155, 27.6%) and cell migration (GO: 0016477, 14.5%) (**Figures 2A, S3A, Table S4-5**). The unsupervised cluster analysis shows the distribution of the 381 differentially expressed proteins in $MKN1^{OE}$ in comparison to $MKN1^{PAR}$, proteins involved in cell migration or cell adhesion biological processes are high-lighted (**Figure 2B**). Refining of the two GO-term hierarchies revealed altered protein abundance in more specific clusters in a pro-tumorigenic way, namely the up-regulation of epithelial cell migration (GO:0010631, p=5.68E-04) and cell-matrix adhesion (GO:0007160, p=0.010), and the down-regulation of leukocyte migration (GO:0050900, p=4.37E-03) and cell adhesion regulation (GO:0045785, p=0.012) (**Figure 2C**). Major altered proteins are basal cell adhesion molecule (BCAM) and collagen type III α1 (COL3A1) (both involved in extracellular matrix (ECM) reorganization) and serine/threonine Ras-activated protein (STRAP) and coronin 1B (CORO1B) which is involved in cell migration and invasion. Down-regulated proteins integrin subunit alpha 2 (ITGA2) and unconventional myosin 1G (MYO1G) (both involved in leukocyte migration), cysteine-rich 61 (CCN1) (ECM-protein regulating cell adhesion), CD59 and CD55 (integrins involved in complement cascade activation) (**Figure 2C**). Most of the aforementioned proteins have been implicated with poor prognosis and metastasis in gastro-intestinal cancers.[105–109]
We next questioned whether sEV derived from $MKN1^{OE}$ could indeed functionally regulate cell migration. Indeed, $MKN1^{OE}$-sEVs increased cell migration of $MKN1^{PAR}$ cells, compared to $MKN1^{PAR}$-sEVs (**Figures 2D-E**). In contrast, large EVs collected from $MKN1^{PAR}$ and $MKN1^{OE}$ cells were unable to induce migration in recipient cells (**Figures S3B-C**). In addition, co-culture migration experiments with $MKN1^{PAR}$ or $MKN1^{OE}$ cells showed that factors present in the $MKN1^{OE}$ secretome can induce migration in recipient (non) cancer cell lines (**Figures S3E-F**). Thus, our data suggest that DCLK1 reprograms the secretome and more specifically sEVs, to support a pro-migratory phenotype in recipient cells.

Molecular inhibition of DCLK1 identifies 61 altered sEV cargo proteins.

To understand DCLK1 kinase-dependent cargo selection for sEVs, we compared the proteome profiling between $MKN1^{OE}$ and $MKN1^{OE+INH}$ sEVs. Across the 1400 identified proteins, this revealed 61 proteins with altered abundance (students t-test $p<0.05$), including 16 up-regulated and 45 down-regulated proteins (**Figure 3A, Tables S6-7**). Interestingly, 31% of these proteins are associated with cell adhesion (GO:0007155, 21%) and/or cell migration (GO: 0016477, 18%) (**Figures 3A, S3D, Tables S8-9**), supporting a functional association of DCKL1 with these cellular processes. Among the proteins displaying a DCLK1-kinase activity dependent abundance (**Figure 3B**), we identified CCN1, KTN1, STRAP, RCC2, SBDS and JAK1 that collectively have been implicated previously with cell migration, EMT or ECM regulation in gastric or other malignancies.[110–114]

Identification of 55 DCLK1-kinase dependent sEV cargo proteins

We next questioned the association of DCLK1 activity with the sEV proteome – looking whether the 61 altered sEV proteins upon DCLK1 inhibition are also altered upon overexpression. We performed a correlation analysis of these differentially expressed components in sEVs ($MKN1^{OE}/MKN1^{PAR}$ vs $MKN1^{OE+INH}/MKN1^{OE}$) revealing a strong negative correlation (R^2=-0.745, p = 5.37e-12, Pearson correlation) and resulting in 55/61 proteins that are altered in a kinase dependent way (**Figure 3C, Table S6**). Of which 13 are down-regulated upon overexpression ($MKN1^{OE}/MKN1^{PAR}$) and up-regulated upon DCLK1 inhibition ($MKN1^{OE+INH}/MKN1^{OE}$) and vice versa 45 proteins are up and then

down regulated, respectively. Two key proteins up-regulated upon DCLK1 overexpression and down-regulated upon inhibition (up – down) include DEK (oncoprotein associated with chromatin organization) and KTN1 (microtubule-based movement, adhesion and migration), while opposite behaving (down - up) proteins include the ECM binding protein CCN1 (associated with cell proliferation and cell adhesion) and endosomal sorting protein CHMP1A (**Figure 3C**). The heatmap reveals that the $MKN1^{PAR}$ and $MKN1^{OE+INH}$ replicates cluster together separate of the $MKN1^{OE}$ replicates, indicating the inhibition of DCLK1 brings these protein levels down to baseline ($MKN1^{PAR}$) (**Figure 3D**). Interestingly, 15/55 proteins are associated with cell adhesion and/or cell migration. Thus, it appears that DCLK1 can modulate the composition of sEVs in a kinase-dependent manner, resulting in key changes in pro-adhesive and pro-migratory factors, supported by the known functions of DCLK1 in cell migration and adhesion as mentioned above.

Discussion

In this study, we establish a new functional role for the DCLK1 in supporting sEV biogenesis, secretion and reprogramming sEV cargo towards a pro-migratory phenotype, *in vitro*. This is in line with previous reports linking DCLK1 expression to the induction of signaling pathways effecting cancer cell motility, invasion and EMT.[7,8,10,13,19,20,22,23,115] Our results also align and extend mechanistic models of DCLK1 as a polymerizer and stabilizer of microtubules and therefore facilitator of vesicular trafficking.[31,32,39,41,45,116]

The exact mechanisms of DCLK1 altering EV biogenesis or influencing cargo selection is currently unknown. Nevertheless, the reversible nature of sEV size, cargo quantity and composition after DCLK1 kinase inhibition is a clear indicator of an important role for the catalytic activity of DCLK1 in all or some of these processes. Whilst our sEV proteome analysis is of limited use in deciphering the intracellular processes associated with localization/trafficking and directly regulated by DCLK1, it has uncovered several candidates that may explain the promotion of EV biogenesis in DCLK1 overexpressing cells (**Figure 4A**). Most intriguingly is Kinectin (KTN1), an organelle trans-membrane receptor involved in intracellular organelle motility.[117,118] KTN1 anchors vesicles and organelles to kinesins, which are transported towards the plus-ends of the microtubules.[119] Further, binding of KTN1 to kinesin stimulates kinesin-ATPase activity, releasing kinesin from its inactive compact formation.[120] This observation is consistent with the known localization of DCLK1 at the plus-ends of microtubules and doublecortin-stabilized microtubules are substrates for kinesin translocase motors and for depolymerase kinesins.[36,37] The combination of both increased DCLK1 and KTN1 levels could be a mechanism through which kinesins are facilitated to bind to both the microtubules and the vesicles, increasing vesicular and organelle transport stability and rate. This could explain the increased amount of secreted sEVs *in vitro*. Another explanation for this might be the reduction of MYO1G, which has been shown to be essential for lysosome stability in different human cancer cell types.[121] The down-regulation of MYO1G and probable destabilization of the lysosome might influence the decision of MVBs being fused to the plasma membrane rather than with the lysosome.[58] In contrast, charged multivesicular body protein 1A (CHMP1A), is a protein which, in yeast, has been shown to directly interact with vacuolar protein sorting 4 (VPS4), [122] a component of the endosomal sorting complex required for transport III (ESCRT-III), which is mainly responsible for scission of the intraluminal vesicles (ILVs) into the MVBs.[122] This might suggest that a lack of

CHMP1A may cause delays in scission leading to potential defects in the generation of MVBs and may help explain the larger vesicles observed after forced DCLK1 expression and their reversion to normal size after inhibitor treatment. Indeed, such findings are supported by a report where membrane properties and heterogeneity of melanoma-derived EVs is influenced by membrane organization and sorting machineries.[123] The involvement of DCLK1 in vesicle-mediated transport pathways is supported by four recent LC-MS/MS studies investigating DCLK1 function by overexpression and/or inhibition, affinity purifications and *in vitro* kinase-assays (**Table S10**).[89,115,124,125] A reactome pathway analysis reveals that 3-7% of significantly altered (phospho) proteins or affinity-purified DCLK1 interacting proteins are associated with vesicle-mediated transport (**Figures S4A-B**). This supports a more general role for DCLK1 involvement, either directly or indirectly, in EV-trafficking and biogenesis.

Several studies have shown that high expression of DCLK1 induces EMT and increases migration and invasion in several different cancer types through various mechanisms. [7,8,10,13,19,20,22,23] In this study, in addition to identifying up-regulated pro-migratory cargo proteins within sEVs from DCLK1 overexpressing MKN1 cells, we also show that these sEVs indeed increase cell migration of MKN1 parental cells *in vitro*. Thus revealing an as of yet unappreciated role for DCLK1 indirectly reprogramming recipient cells. Two most interesting kinase dependent cargo proteins associated with epithelial cell migration are coronin 1B (CORO1B) and serine/threonine kinase receptor-associated protein (STRAP), both are increased in $MKN1^{OE}$-sEVs and decreased in $MKN1^{OE+INH}$-EVs (**Figure 4B**). CORO1B regulates various actin-dependent cellular processes via Arp2/3 complex interactions promoting cell protrusion, migration and scission.[126] Silenced or kinase dead CORO1B has been shown to reduce migration in a multitude of different cancer and non-cancer cells.[126–129] In addition, type I cornonins have been associated with poor prognosis and metastasis in GC.[130,131] Interestingly, STRAP is also significantly up-regulated in GCs compared to adjacent normal tissue and STRAP silencing has been shown to reduce cell migration and invasion *in vitro,* and metastasis *in vivo* in CRC and osteosarcoma.[108,132,133] A different study showed that STRAP is tethered to collagen mRNAs and facilitates its translation and thus indirectly regulating ECM stiffness and cell-matrix adhesion.[134] Stiffening of the ECM induces focal adhesion formations within the cells, which are essential for directional cancer cell motility.[135–137]

As well as pro-migratory proteins, the sEVs released by $MKN1^{OE}$ cells also carried more abundant cell-matrix adhesion promoting proteins, of which BCAM and COL3A1 are the top two associated proteins (**Figure 4C**). BCAM is a member of the immunoglobulin superfamily and a receptor for the ECM protein laminin. Interestingly, BCAM levels are significantly higher in primary GC tumors of patients with metastasis and predict a worse overall survival and increase cell migration, invasion and metastasis by mediating tumor-ECM interactions.[105,138] COL3A1 is a type III collagen and part of the interstitial matrix regulating stromal components and is up-regulated in GC versus normal stomach tissue and is a marker of poor prognosis in many cancer types.[106,107,139,140] ECM protein CCN1 is a DCLK1 kinase-dependent sEV cargo protein and is down-regulated upon overexpression and up-regulated upon inhibition. CCN1 is secreted into the ECM regulating a broad spectrum of cellular activities, including cell adhesion and migration in a cell type and context dependent manner.[114,141–143] High CCN1 levels are linked to sites of inflammation and wound healing processes, activation of NFκB signalling in macrophages polarizing them towards a pro-

inflammatory M1 phenotype and can induce cell type specific apoptosis of fibroblasts through the activation of FasL, TNFα or integrins.[142,144,145] The down-regulation of CCN1, and up-regulation of BCAM and COL3A1 upon DCLK1 overexpression is suggestive of a cell extrinsic role for DCLK1 in the regulation of immune evasive, matrix stiffening, pro-migratory and pro-fibroblastic processes.

A limiting factor of this study is the use of only a single cell line. Future work should investigate whether the same effects on EV-biogenesis and EV cargo selection are observed in other (non)-cancerous cell lines after forced expression of DCLK1. Nevertheless, large proteomic datasets investigating DCLK1 function support a more general role for DCLK1 in vesicle-mediated transport (**Figures S4A-B**), suggesting that our observations in MKN1 cells are not restricted to a particular cell type. However, whether MKN1^{OE}-derived sEVs rather than other factors in the total cell secretome, have the ability to promote migration of cells needs to be investigated in order to assess whether this is a cell-type specific or more stereotyped output. In this study, we show that the *in vitro* pro-migratory reprogramming of EVs is not conserved among all types of EVs but rather restricted to sEVs.

In conclusion, our data has uncovered a novel role for DCLK1 in sEV biogenesis. We found kinase-dependent and independent functions for DCLK1 in sEV biology relating to size, composition and secretion. One of the principal impacts of DCLK1-reprogrammed sEVs is the ability to promote cell migration in recipient cells, *in vitro*. Other altered cargo proteins are associated with GO biological processes that weaken cell-cell adhesion, strengthen cell-matrix adhesion and influence leukocyte migration. These novel insights into DCLK1 function may pave the way for a better understanding of its role as a maker of cancer stem cells and driver of tumorigenesis.

Data Availability Statement

The data that support the findings of this study are openly available in ProteomeXchange Consortium via the PRIDE at https://www.ebi.ac.uk/pride/archive, reference number PXD021371.

References

[1] Sossey-Alaoui, K., & Srivastava, A. K. (1999). DCAMKL1, a brain-specific transmembrane protein on 13q12.3 That is similar to doublecortin (DCX). *Genomics*, *56*(1), 121–126.

[2] Matsumoto, N., Pilz, D. T., & Ledbetter, D. H. (1999). Genomic Structure, Chromosomal Mapping, and Expression Pattern of Human DCAMKL1 (KIAA0369), a Homologue of DCX (XLIS). *Genomics*, *56*(2), 179–183.

[3] Lin, P. T., Gleeson, J. G., Corbo, J. C., Flanagan, L., & Walsh, C. A. (2000). DCAMKL1 encodes a protein kinase with homology to doublecortin that regulates microtubule polymerization. *The Journal of Neuroscience : The Official Journal of the Society for Neuroscience*, *20*(24), 9152–9161.

[4] Westphalen, C. B., Asfaha, S., Hayakawa, Y., Takemoto, Y., Lukin, D. J., Nuber, A. H., Brandtner, A.,

Setlik, W., Remotti, H., Muley, A., Chen, X., May, R., Houchen, C. W., Fox, J. G., Gershon, M. D., Quante, M., & Wang, T. C. (2014). Long-lived intestinal tuft cells serve as colon cancer–initiating cells. *Journal of Clinical Investigation*, *124*(3), 1283–1295.

[5] Nakanishi, Y., Seno, H., Fukuoka, A., Ueo, T., Yamaga, Y., Maruno, T., Nakanishi, N., Kanda, K., Komekado, H., Kawada, M., Isomura, A., Kawada, K., Sakai, Y., Yanagita, M., Kageyama, R., Kawaguchi, Y., Taketo, M. M., Yonehara, S., & Chiba, T. (2013). Dclk1 distinguishes between tumor and normal stem cells in the intestine. *Nature Genetics*, *45*(1), 98–103.

[6] May, R., Riehl, T. E., Hunt, C., Sureban, S. M., Anant, S., & Houchen, C. W. (2008). Identification of a novel putative gastrointestinal stem cell and adenoma stem cell marker, doublecortin and CaM kinase-like-1, following radiation injury and in adenomatous polyposis coli/multiple intestinal neoplasia mice. *Stem Cells (Dayton, Ohio)*, *26*(3), 630–637.

[7] Makino, S., Takahashi, H., Okuzaki, D., Miyoshi, N., Haraguchi, N., Hata, T., Matsuda, C., Yamamoto, H., Mizushima, T., Mori, M., & Doki, Y. (2020). DCLK1 integrates induction of TRIB3, EMT, drug resistance and poor prognosis in colorectal cancer. *Carcinogenesis*, *41*(3), 303–312.

[8] Liu, Z.-Q., He, W.-F., Wu, Y.-J., Zhao, S.-L., Wang, L., Ouyang, Y.-Y., & Tang, S.-Y. (2020). LncRNA SNHG1 promotes EMT process in gastric cancer cells through regulation of the miR-15b/DCLK1/Notch1 axis. *BMC Gastroenterology*, *20*(1), 156.

[9] Qiu, W., Remotti, H. E., Tang, S. M., Wang, E., Dobberteen, L., Lee Youssof, A., Lee, J. H., Cheung, E. C., & Su, G. H. (2018). Pancreatic DCLK1+ cells originate distinctly from PDX1+ progenitors and contribute to the initiation of intraductal papillary mucinous neoplasm in mice. *Cancer Letters*, *423*, 71–79.

[10] Liu, W., Wang, S., Sun, Q., Yang, Z., Liu, M., & Tang, H. (2018). DCLK1 promotes epithelial-mesenchymal transition via the PI3K/Akt/NF-κB pathway in colorectal cancer. *International Journal of Cancer*, *142*(10), 2068–2079.

[11] Ge, Y., Weygant, N., Qu, D., May, R., Berry, W. L., Yao, J., Chandrakesan, P., Zheng, W., Zhao, L., Zhao, K. L., Drake, M., Vega, K. J., Bronze, M. S., Tomasek, J. J., An, G., & Houchen, C. W. (2018). Alternative splice variants of DCLK1 mark cancer stem cells, promote self-renewal and drug-resistance, and can be targeted to inhibit tumorigenesis in kidney cancer. *International Journal of Cancer*, *143*(5), 1162–1175.

[12] Sarkar, S., O'Connell, M. R., Okugawa, Y., Lee, B. S., Toiyama, Y., Kusunoki, M., Daboval, R. D., Goel, A., & Singh, P. (2017). FOXD3 Regulates CSC Marker, DCLK1-S, and Invasive Potential: Prognostic Implications in Colon Cancer. *Molecular Cancer Research : MCR*, *15*(12), 1678–1691.

[13] Chandrakesan, P, Panneerselvam, J., Qu, D., Weygant, N., May, R., Bronze, M. S., & Houchen, C. W. (2016). Regulatory Roles of Dclk1 in Epithelial Mesenchymal Transition and Cancer Stem Cells. *Journal of Carcinogenesis & Mutagenesis*, *7*(2).

[14] Mirzaei, A., Madjd, Z., Kadijani, A. A., Tavakoli-Yaraki, M., Modarresi, M. H., Verdi, J., Akbari, A., & Tavoosidana, G. (2016). Evaluation of circulating cellular DCLK1 protein, as the most promising colorectal cancer stem cell marker, using immunoassay based methods. *Cancer Biomarkers : Section*

A of Disease Markers, *17*(3), 301–311.

[15] Mirzaei, A., Tavoosidana, G., Modarressi, M. H., Rad, A. A., Fazeli, M. S., Shirkoohi, R., Tavakoli-Yaraki, M., & Madjd, Z. (2015). Upregulation of circulating cancer stem cell marker, DCLK1 but not Lgr5, in chemoradiotherapy-treated colorectal cancer patients. *Tumour Biology : The Journal of the International Society for Oncodevelopmental Biology and Medicine*, *36*(6), 4801–4810.

[16] Koga, H., Ikezono, Y., & Torimura, T. (2016). Pancreatic DCLK1 marks quiescent but oncogenic progenitors: a possible link to neuroendocrine tumors. *Stem Cell Investigation*, *3*, 37.

[17] Ito, H., Tanaka, S., Akiyama, Y., Shimada, S., Adikrisna, R., Matsumura, S., Aihara, A., Mitsunori, Y., Ban, D., Ochiai, T., Kudo, A., Arii, S., Yamaoka, S., & Tanabe, M. (2016). Dominant Expression of DCLK1 in Human Pancreatic Cancer Stem Cells Accelerates Tumor Invasion and Metastasis. *PloS One*, *11*(1), e0146564.

[18] Qu, D., May, R., Sureban, S. M., Weygant, N., Chandrakesan, P., Ali, N., Li, L., Barrett, T., & Houchen, C. W. (2014). Inhibition of Notch signaling reduces the number of surviving Dclk1+ reserve crypt epithelial stem cells following radiation injury. *American Journal of Physiology. Gastrointestinal and Liver Physiology*, *306*(5), G404-11.

[19] Ikezono, Y., Koga, H., Akiba, J., Abe, M., Yoshida, T., Wada, F., Nakamura, T., Iwamoto, H., Masuda, A., Sakaue, T., Yano, H., Tsuruta, O., & Torimura, T. (2017). Pancreatic Neuroendocrine Tumors and EMT Behavior Are Driven by the CSC Marker DCLK1. *Molecular Cancer Research : MCR*, *15*(6), 744–752.

[20] Weygant, N., Qu, D., May, R., Tierney, R. M., Berry, W. L., Zhao, L., Agarwal, S., Chandrakesan, P., Chinthalapally, H. R., Murphy, N. T., Li, J. D., Sureban, S. M., Schlosser, M. J., Tomasek, J. J., & Houchen, C. W. (2015). DCLK1 is a broadly dysregulated target against epithelial-mesenchymal transition, focal adhesion, and stemness in clear cell renal carcinoma. *Oncotarget*, *6*(4), 2193–2205.

[21] Chandrakesan, Parthasarathy, Yao, J., Qu, D., May, R., Weygant, N., Ge, Y., Ali, N., Sureban, S. M., Gude, M., Vega, K., Bannerman-Menson, E., Xia, L., Bronze, M., An, G., & Houchen, C. W. (2017). Dclk1, a tumor stem cell marker, regulates pro-survival signaling and self-renewal of intestinal tumor cells. *Molecular Cancer*, *16*(1), 30.

[22] Sureban, S. M., May, R., Lightfoot, S. A., Hoskins, A. B., Lerner, M., Brackett, D. J., Postier, R. G., Ramanujam, R., Mohammed, A., Rao, C. V, Wyche, J. H., Anant, S., & Houchen, C. W. (2011). DCAMKL-1 regulates epithelial-mesenchymal transition in human pancreatic cells through a miR-200a-dependent mechanism. *Cancer Research*, *71*(6), 2328–2338.

[23] Chandrakesan, Parthasarathy, Weygant, N., May, R., Qu, D., Chinthalapally, H. R., Sureban, S. M., Ali, N., Lightfoot, S. A., Umar, S., & Houchen, C. W. (2014). DCLK1 facilitates intestinal tumor growth via enhancing pluripotency and epithelial mesenchymal transition. *Oncotarget*, *5*(19), 9269–9280.

[24] Panneerselvam, J., Mohandoss, P., Patel, R., Gillan, H., Li, M., Kumar, K., Nguyen, D., Weygant, N., Qu, D., Pitts, K., Lightfoot, S., Rao, C., Houchen, C., Bronze, M., & Chandrakesan, P. (2020). DCLK1 Regulates Tumor Stemness and Cisplatin Resistance in Non-small Cell Lung Cancer via ABCD-

Member-4. *Molecular Therapy Oncolytics*, *18*, 24–36.

[25] Kadletz, L., Kenner, L., Wiebringhaus, R., Jank, B., Mayer, C., Gurnhofer, E., Konrad, S., & Heiduschka, G. (2019). Evaluation of the cancer stem cell marker DCLK1 in patients with lymph node metastases of head and neck cancer. *Pathology, Research and Practice*, *215*(12), 152698.

[26] Wang, K., Yuen, S. T., Xu, J., Lee, S. P., Yan, H. H. N., Shi, S. T., Siu, H. C., Deng, S., Chu, K. M., Law, S., Chan, K. H., Chan, A. S. Y., Tsui, W. Y., Ho, S. L., Chan, A. K. W., Man, J. L. K., Foglizzo, V., Ng, M. K., Chan, A. S., … Leung, S. Y. (2014). Whole-genome sequencing and comprehensive molecular profiling identify new driver mutations in gastric cancer. *Nature Genetics*, *46*(6), 573–582.

[27] Yan, R., Li, J., Zhou, Y., Yao, L., Sun, R., Xu, Y., Ge, Y., & An, G. (2020). Inhibition of DCLK1 down-regulates PD-L1 expression through Hippo pathway in human pancreatic cancer. *Life Sciences*, *241*, 117150.

[28] Wu, X., Qu, D., Weygant, N., Peng, J., & Houchen, C. W. (2020). Cancer Stem Cell Marker DCLK1 Correlates with Tumorigenic Immune Infiltrates in the Colon and Gastric Adenocarcinoma Microenvironments. *Cancers*, *12*(2), 274.

[29] Akhmanova, A., & Steinmetz, M. O. (2015). Control of microtubule organization and dynamics: two ends in the limelight. *Nature Reviews Molecular Cell Biology*, *16*(12), 711–726.

[30] Mohan, R., & John, A. (2015). Microtubule-associated proteins as direct crosslinkers of actin filaments and microtubules. *IUBMB Life*, *67*(6), 395–403.

[31] Reiner, O., Coquelle, F. M., Peter, B., Levy, T., Kaplan, A., Sapir, T., Orr, I., Barkai, N., Eichele, G., & Bergmann, S. (2006). The evolving doublecortin (DCX) superfamily. *BMC Genomics*, *7*(1), 188.

[32] Coquelle, F. M., Levy, T., Bergmann, S., Wolf, S. G., Bar-El, D., Sapir, T., Brody, Y., Orr, I., Barkai, N., Eichele, G., & Reiner, O. (2006). The DCX Superfamily 1: Common and Divergent Roles for Members of the Mouse DCX Superfamily. *Cell Cycle*, *5*(9), 976–983.

[33] Al-Bassam, J., Ozer, R. S., Safer, D., Halpain, S., & Milligan, R. A. (2002). MAP2 and tau bind longitudinally along the outer ridges of microtubule protofilaments. *J Cell Biol*, *157*(7), 1187–1196.

[34] Bechstedt, S., Lu, K., & Brouhard, G. J. (2014). Doublecortin recognizes the longitudinal curvature of the microtubule end and lattice. *Current Biology : CB*, *24*(20), 2366–2375.

[35] Bechstedt, S., & Brouhard, G. J. (2012). Doublecortin recognizes the 13-protofilament microtubule cooperatively and tracks microtubule ends. *Developmental Cell*, *23*(1), 181–192.

[36] Moores, C. A., Perderiset, M., Francis, F., Chelly, J., Houdusse, A., & Milligan, R. A. (2004). Mechanism of Microtubule Stabilization by Doublecortin. *Molecular Cell*, *14*(6), 833–839.

[37] Moores, C. A., Perderiset, M., Kappeler, C., Kain, S., Drummond, D., Perkins, S. J., Chelly, J., Cross, R., Houdusse, A., & Francis, F. (2006). Distinct roles of doublecortin modulating the microtubule cytoskeleton. *The EMBO Journal*, *25*(19), 4448–4457.

[38] Kim, M. H., Cierpicki, T., Derewenda, U., Krowarsch, D., Feng, Y., Devedjiev, Y., Dauter, Z., Walsh, C. A., Otlewski, J., Bushweller, J. H., & Derewenda, Z. S. (2003). The DCX-domain tandems of

doublecortin and doublecortin-like kinase. *Nature Structural Biology*, *10*(5), 324–333.

[39] Patel, O., Dai, W., Mentzel, M., Griffin, M. D. W., Serindoux, J., Gay, Y., Fischer, S., Sterle, S., Kropp, A., Burns, C. J., Ernst, M., Buchert, M., & Lucet, I. S. (2016). Biochemical and Structural Insights into Doublecortin-like Kinase Domain 1. *Structure*, 1–12.

[40] Friocourt, G., Koulakoff, A., Chafey, P., Boucher, D., Fauchereau, F., Chelly, J., & Francis, F. (2003). Doublecortin functions at the extremities of growing neuronal processes. *Cerebral Cortex (New York, N.Y. : 1991)*, *13*(6), 620–626.

[41] Deuel, T. A. S., Liu, J. S., Corbo, J. C., Yoo, S.-Y., Rorke-Adams, L. B., & Walsh, C. A. (2006). Genetic interactions between doublecortin and doublecortin-like kinase in neuronal migration and axon outgrowth. *Neuron*, *49*(1), 41–53.

[42] Schenk, G. J., Engels, B., Zhang, Y.-P., Fitzsimons, C. P., Schouten, T., Kruidering, M., de Kloet, E. R., & Vreugdenhil, E. (2007). A potential role for calcium / calmodulin-dependent protein kinase-related peptide in neuronal apoptosis: in vivo and in vitro evidence. *The European Journal of Neuroscience*, *26*(12), 3411–3420.

[43] Wu, J. Q., Wang, X., Beveridge, N. J., Tooney, P. A., Scott, R. J., Carr, V. J., & Cairns, M. J. (2012). Transcriptome sequencing revealed significant alteration of cortical promoter usage and splicing in schizophrenia. *PloS One*, *7*(4), e36351.

[44] Liu, J. S., Schubert, C. R., Fu, X., Fourniol, F. J., Jaiswal, J. K., Houdusse, A., Stultz, C. M., Moores, C. A., & Walsh, C. A. (2012). Molecular basis for specific regulation of neuronal kinesin-3 motors by doublecortin family proteins. *Molecular Cell*, *47*(5), 707–721.

[45] Lipka, J., Kapitein, L. C., Jaworski, J., & Hoogenraad, C. C. (2016). Microtubule-binding protein doublecortin-like kinase 1 (DCLK1) guides kinesin-3-mediated cargo transport to dendrites. *The EMBO Journal*, *35*(3), 302–318.

[46] Creaney, J., Dick, I. M., Leon, J. S., & Robinson, B. W. S. (n.d.-at). A Proteomic Analysis of the Malignant Mesothelioma Secretome Using iTRAQ. *Cancer Genomics & Proteomics*, *14*(2), 103–117.

[47] Mustafa, S., Pan, L., Marzoq, A., Fawaz, M., Sander, L., Rückert, F., Schrenk, A., Hartl, C., Uhler, R., Yildirim, A., Strobel, O., Hackert, T., Giese, N., Büchler, M. W., Hoheisel, J. D., & Alhamdani, M. S. S. (2017). Comparison of the tumor cell secretome and patient sera for an accurate serum-based diagnosis of pancreatic ductal adenocarcinoma. *Oncotarget*, *8*(7), 11963–11976.

[48] Ziegler, Y. S., Moresco, J. J., Yates, J. R., & Nardulli, A. M. (2016). Integration of Breast Cancer Secretomes with Clinical Data Elucidates Potential Serum Markers for Disease Detection, Diagnosis, and Prognosis. *PloS One*, *11*(6), e0158296.

[49] Prieto-García, E., Díaz-García, C. V., Agudo-López, A., Pardo-Marqués, V., García-Consuegra, I., Asensio-Peña, S., Alonso-Riaño, M., Pérez, C., Gómez, C., Adeva, J., Paz-Ares, L., López-Martín, J. A., & Agulló-Ortuño, M. T. (2021). Tumor-Stromal Interactions in a Co-Culture Model of Human Pancreatic Adenocarcinoma Cells and Fibroblasts and Their Connection with Tumor Spread. *Biomedicines*, *9*(4).

[50] Dörsam, B., Bösl, T., Reiners, K. S., Barnert, S., Schubert, R., Shatnyeva, O., Zigrino, P., Engert, A., Hansen, H. P., & von Strandmann, E. P. (2018). Hodgkin Lymphoma-Derived Extracellular Vesicles Change the Secretome of Fibroblasts Toward a CAF Phenotype. *Frontiers in Immunology*, *9*, 1358.

[51] Dieters-Castator, D., Dantonio, P. M., Piaseczny, M., Zhang, G., Liu, J., Kuljanin, M., Sherman, S., Jewer, M., Quesnel, K., Kang, E. Y., Köbel, M., Siegers, G. M., Leask, A., Hess, D., Lajoie, G., & Postovit, L.-M. (2021). Embryonic protein NODAL regulates the breast tumor microenvironment by reprogramming cancer-derived secretomes. *Neoplasia (New York, N.Y.)*, *23*(4), 375–390.

[52] Heeran, A. B., Dunne, M. R., Morrissey, M. E., Buckley, C. E., Clarke, N., Cannon, A., Donlon, N. E., Nugent, T. S., Durand, M., Dunne, C., Larkin, J. O., Mehigan, B., McCormick, P., Lynam-Lennon, N., & O'Sullivan, J. (2021). The Protein Secretome Is Altered in Rectal Cancer Tissue Compared to Normal Rectal Tissue, and Alterations in the Secretome Induce Enhanced Innate Immune Responses. *Cancers*, *13*(3).

[53] Ritchie, S., Reed, D. A., Pereira, B. A., & Timpson, P. (2021). The cancer cell secretome drives cooperative manipulation of the tumour microenvironment to accelerate tumourigenesis. *Faculty Reviews*, *10*, 4.

[54] López de Andrés, J., Griñán-Lisón, C., Jiménez, G., & Marchal, J. A. (2020). Cancer stem cell secretome in the tumor microenvironment: a key point for an effective personalized cancer treatment. *Journal of Hematology & Oncology*, *13*(1), 136.

[55] Greening, D. W., & Simpson, R. J. (2018). Understanding extracellular vesicle diversity–current status. *Expert Review of Proteomics*, *15*(11), 887–910.

[56] Tricarico, C., Clancy, J., & D'Souza-Schorey, C. (2017). Biology and biogenesis of shed microvesicles. *Small GTPases*, *8*(4), 220–232.

[57] Muralidharan-Chari, V., Clancy, J. W., Sedgwick, A., & D'Souza-Schorey, C. (2010). Microvesicles: mediators of extracellular communication during cancer progression. *Journal of Cell Science*, *123*(Pt 10), 1603–1611.

[58] Van Niel, G., D'Angelo, G., & Raposo, G. (2018). Shedding light on the cell biology of extracellular vesicles. *Nature Reviews. Molecular Cell Biology*, *19*(4), 213–228.

[59] Haraszti, R. A., Didiot, M.-C., Sapp, E., Leszyk, J., Shaffer, S. A., Rockwell, H. E., Gao, F., Narain, N. R., DiFiglia, M., Kiebish, M. A., Aronin, N., & Khvorova, A. (2016). High-resolution proteomic and lipidomic analysis of exosomes and microvesicles from different cell sources. *Journal of Extracellular Vesicles*, *5*(1), 32570.

[60] Tang, Z., Li, D., Hou, S., & Zhu, X. (2020). The cancer exosomes: Clinical implications, applications and challenges. *International Journal of Cancer*, *146*(11), 2946–2959.

[61] Pegtel, D. M., & Gould, S. J. (2019). Exosomes. *Annual Review of Biochemistry*, *88*, 487–514.

[62] Rai, A., Greening, D. W., Xu, R., Chen, M., Suwakulsiri, W., & Simpson, R. J. (2021). Secreted midbody remnants are a class of extracellular vesicles molecularly distinct from exosomes and microparticles. *Communications Biology*, *4*(1), 400.

[63] Ettinger, A. W., Wilsch-Bräuninger, M., Marzesco, A.-M., Bickle, M., Lohmann, A., Maliga, Z., Karbanová, J., Corbeil, D., Hyman, A. A., & Huttner, W. B. (2011). Proliferating versus differentiating stem and cancer cells exhibit distinct midbody-release behaviour. *Nature Communications*, *2*, 503.

[64] Zhang, H., Freitas, D., Kim, H. S., Fabijanic, K., Li, Z., Chen, H., Mark, M. T., Molina, H., Martin, A. B., Bojmar, L., Fang, J., Rampersaud, S., Hoshino, A., Matei, I., Kenific, C. M., Nakajima, M., Mutvei, A. P., Sansone, P., Buehring, W., … Lyden, D. (2018). Identification of distinct nanoparticles and subsets of extracellular vesicles by asymmetric flow field-flow fractionation. *Nature Cell Biology*, *20*(3), 332–343.

[65] Zhang, Q., Higginbotham, J. N., Jeppesen, D. K., Yang, Y.-P., Li, W., McKinley, E. T., Graves-Deal, R., Ping, J., Britain, C. M., Dorsett, K. A., Hartman, C. L., Ford, D. A., Allen, R. M., Vickers, K. C., Liu, Q., Franklin, J. L., Bellis, S. L., & Coffey, R. J. (2019). Transfer of Functional Cargo in Exomeres. *Cell Reports*, *27*(3), 940-954.e6.

[66] Witwer, K. W., & Théry, C. (2019). Extracellular vesicles or exosomes? On primacy, precision, and popularity influencing a choice of nomenclature. *Journal of Extracellular Vesicles*, *8*(1), 1648167.

[67] Gould, S. J., & Raposo, G. (2013). As we wait: coping with an imperfect nomenclature for extracellular vesicles. *Journal of Extracellular Vesicles*, *2*.

[68] Théry, C., Witwer, K. W., Aikawa, E., Alcaraz, M. J., Anderson, J. D., Andriantsitohaina, R., Antoniou, A., Arab, T., Archer, F., Atkin-Smith, G. K., Ayre, D. C., Bach, J.-M., Bachurski, D., Baharvand, H., Balaj, L., Baldacchino, S., Bauer, N. N., Baxter, A. A., Bebawy, M., … Zuba-Surma, E. K. (2018). Minimal information for studies of extracellular vesicles 2018 (MISEV2018): a position statement of the International Society for Extracellular Vesicles and update of the MISEV2014 guidelines. *Journal of Extracellular Vesicles*, *7*(1), 1535750.

[69] Greening, D. W., & Simpson, R. J. (2018). Understanding extracellular vesicle diversity - current status. *Expert Review of Proteomics*, *15*(11), 887–910.

[70] Chen, M., Xu, R., Rai, A., Suwakulsiri, W., Izumikawa, K., Ishikawa, H., Greening, D. W., Takahashi, N., & Simpson, R. J. (2019). Distinct shed microvesicle and exosome microRNA signatures reveal diagnostic markers for colorectal cancer. *PloS One*, *14*(1), e0210003.

[71] Jeppesen, D. K., Fenix, A. M., Franklin, J. L., Higginbotham, J. N., Zhang, Q., Zimmerman, L. J., Liebler, D. C., Ping, J., Liu, Q., Evans, R., Fissell, W. H., Patton, J. G., Rome, L. H., Burnette, D. T., & Coffey, R. J. (2019). Reassessment of Exosome Composition. *Cell*, *177*(2), 428-445.e18.

[72] Xu, R., Greening, D. W., Rai, A., Ji, H., & Simpson, R. J. (2015). Highly-purified exosomes and shed microvesicles isolated from the human colon cancer cell line LIM1863 by sequential centrifugal ultrafiltration are biochemically and functionally distinct. *Methods (San Diego, Calif.)*, *87*, 11–25.

[73] Xu, R., Rai, A., Chen, M., Suwakulsiri, W., Greening, D. W., & Simpson, R. J. (2018). Extracellular vesicles in cancer - implications for future improvements in cancer care. *Nature Reviews. Clinical Oncology*, *15*(10), 617–638.

[74] Rai, A., Greening, D. W., Chen, M., Xu, R., Ji, H., & Simpson, R. J. (2019). Exosomes Derived from Human Primary and Metastatic Colorectal Cancer Cells Contribute to Functional Heterogeneity of

Activated Fibroblasts by Reprogramming Their Proteome. *Proteomics*, *19*(8), e1800148.

[75] Carrasco-Ramírez, P., Greening, D. W., Andrés, G., Gopal, S. K., Martín-Villar, E., Renart, J., Simpson, R. J., & Quintanilla, M. (2016). Podoplanin is a component of extracellular vesicles that reprograms cell-derived exosomal proteins and modulates lymphatic vessel formation. *Oncotarget*, *7*(13), 16070–16089.

[76] Greening, D. W., Gopal, S. K., Xu, R., Simpson, R. J., & Chen, W. (2015). Exosomes and their roles in immune regulation and cancer. *Seminars in Cell & Developmental Biology*, *40*, 72–81.

[77] Peinado, H., Alečković, M., Lavotshkin, S., Matei, I., Costa-Silva, B., Moreno-Bueno, G., Hergueta-Redondo, M., Williams, C., García-Santos, G., Ghajar, C., Nitadori-Hoshino, A., Hoffman, C., Badal, K., Garcia, B. A., Callahan, M. K., Yuan, J., Martins, V. R., Skog, J., Kaplan, R. N., … Lyden, D. (2012). Melanoma exosomes educate bone marrow progenitor cells toward a pro-metastatic phenotype through MET. *Nature Medicine*, *18*(6), 883–891.

[78] Costa-Silva, B., Aiello, N. M., Ocean, A. J., Singh, S., Zhang, H., Thakur, B. K., Becker, A., Hoshino, A., Mark, M. T., Molina, H., Xiang, J., Zhang, T., Theilen, T.-M., García-Santos, G., Williams, C., Ararso, Y., Huang, Y., Rodrigues, G., Shen, T.-L., … Lyden, D. (2015). Pancreatic cancer exosomes initiate pre-metastatic niche formation in the liver. *Nature Cell Biology*, *17*(6), 816–826.

[79] Hsu, Y.-L., Hung, J.-Y., Chang, W.-A., Lin, Y.-S., Pan, Y.-C., Tsai, P.-H., Wu, C.-Y., & Kuo, P.-L. (2017). Hypoxic lung cancer-secreted exosomal miR-23a increased angiogenesis and vascular permeability by targeting prolyl hydroxylase and tight junction protein ZO-1. *Oncogene*, *36*(34), 4929–4942.

[80] Gopal, S. K., Greening, D. W., Rai, A., Chen, M., Xu, R., Shafiq, A., Mathias, R. A., Zhu, H.-J., & Simpson, R. J. (2017). Extracellular vesicles: their role in cancer biology and epithelial-mesenchymal transition. *The Biochemical Journal*, *474*(1), 21–45.

[81] Liu, C., Yu, S., Zinn, K., Wang, J., Zhang, L., Jia, Y., Kappes, J. C., Barnes, S., Kimberly, R. P., Grizzle, W. E., & Zhang, H.-G. (2006). Murine mammary carcinoma exosomes promote tumor growth by suppression of NK cell function. *Journal of Immunology (Baltimore, Md. : 1950)*, *176*(3), 1375–1385.

[82] Webber, J., Steadman, R., Mason, M. D., Tabi, Z., & Clayton, A. (2010). Cancer exosomes trigger fibroblast to myofibroblast differentiation. *Cancer Research*, *70*(23), 9621–9630.

[83] Webber, J. P., Spary, L. K., Sanders, A. J., Chowdhury, R., Jiang, W. G., Steadman, R., Wymant, J., Jones, A. T., Kynaston, H., Mason, M. D., Tabi, Z., & Clayton, A. (2015). Differentiation of tumour-promoting stromal myofibroblasts by cancer exosomes. *Oncogene*, *34*(3), 290–302.

[84] Wieckowski, E. U., Visus, C., Szajnik, M., Szczepanski, M. J., Storkus, W. J., & Whiteside, T. L. (2009). Tumor-derived microvesicles promote regulatory T cell expansion and induce apoptosis in tumor-reactive activated CD8+ T lymphocytes. *Journal of Immunology (Baltimore, Md. : 1950)*, *183*(6), 3720–3730.

[85] Wortzel, I., Dror, S., Kenific, C. M., & Lyden, D. (2019). Exosome-Mediated Metastasis: Communication from a Distance. *Developmental Cell*, *49*(3), 347–360.

[86] Grange, C., Tapparo, M., Collino, F., Vitillo, L., Damasco, C., Deregibus, M. C., Tetta, C., Bussolati, B., & Camussi, G. (2011). Microvesicles released from human renal cancer stem cells stimulate angiogenesis and formation of lung premetastatic niche. *Cancer Research*, *71*(15), 5346–5356.

[87] Lindoso, R. S., Collino, F., & Camussi, G. (2015). Extracellular vesicles derived from renal cancer stem cells induce a pro-tumorigenic phenotype in mesenchymal stromal cells. *Oncotarget*, *6*(10), 7959–7969.

[88] Mannerström, B., Kornilov, R., Abu-Shahba, A. G., Chowdhury, I. M., Sinha, S., Seppänen-Kaijansinkko, R., & Kaur, S. (2019). Epigenetic alterations in mesenchymal stem cells by osteosarcoma-derived extracellular vesicles. *Epigenetics*, *14*(4), 352–364.

[89] Ferguson, F. M., Nabet, B., Raghavan, S., Liu, Y., Leggett, A. L., Kuljanin, M., Kalekar, R. L., Yang, A., He, S., Wang, J., Ng, R. W. S. S., Sulahian, R., Li, L., Poulin, E. J., Huang, L., Koren, J., Dieguez-Martinez, N., Espinosa, S., Zeng, Z., … Gray, N. S. (2020). Discovery of a selective inhibitor of doublecortin like kinase 1. *Nature Chemical Biology*, *16*(6), 635–643.

[90] Ferguson, F. M., Liu, Y., Harshbarger, W., Huang, L., Wang, J., Deng, X., Capuzzi, S. J., Muratov, E. N., Tropsha, A., Muthuswamy, S., Westover, K. D., & Gray, N. S. (2020). Synthesis and Structure-Activity Relationships of DCLK1 Kinase Inhibitors Based on a 5,11-Dihydro-6H-benzo[e]pyrimido[5,4-b][1,4]diazepin-6-one Scaffold. *Journal of Medicinal Chemistry*, *63*(14), 7817–7826.

[91] Rai, A., Fang, H., Fatmous, M., Claridge, B., Poh, Q. H., Simpson, R. J., & Greening, D. W. (2021). A Protocol for Isolation, Purification, Characterization, and Functional Dissection of Exosomes. *Methods in Molecular Biology (Clifton, N.J.)*, *2261*, 105–149.

[92] Greening, D. W., Xu, R., Ji, H., Tauro, B. J., & Simpson, R. J. (2015). A protocol for exosome isolation and characterization: evaluation of ultracentrifugation, density-gradient separation, and immunoaffinity capture methods. *Methods in Molecular Biology (Clifton, N.J.)*, *1295*, 179–209.

[93] Rai, A., Greening, D. W., Xu, R., Suwakulsiri, W., & Simpson, R. J. (2020). Exosomes Derived from the Human Primary Colorectal Cancer Cell Line SW480 Orchestrate Fibroblast-Led Cancer Invasion. *Proteomics*, *20*(14), e2000016.

[94] Kompa, A. R., Greening, D. W., Kong, A. M., McMillan, P. J., Fang, H., Saxena, R., Wong, R. C. B., Lees, J. G., Sivakumaran, P., Newcomb, A. E., Tannous, B. A., Kos, C., Mariana, L., Loudovaris, T., Hausenloy, D. J., & Lim, S. Y. (2021). Sustained subcutaneous delivery of secretome of human cardiac stem cells promotes cardiac repair following myocardial infarction. *Cardiovascular Research*, *117*(3), 918–929.

[95] Evans, J., Rai, A., Nguyen, H. P. T., Poh, Q. H., Elglass, K., Simpson, R. J., Salamonsen, L. A., & Greening, D. W. (2019). Human Endometrial Extracellular Vesicles Functionally Prepare Human Trophectoderm Model for Implantation: Understanding Bidirectional Maternal-Embryo Communication. *Proteomics*, *19*(23), e1800423.

[96] Cox, J., Neuhauser, N., Michalski, A., Scheltema, R. A., Olsen, J. V, & Mann, M. (2011). Andromeda: a peptide search engine integrated into the MaxQuant environment. *Journal of Proteome Research*, *10*(4), 1794–1805.

[97] Rai, A., Poh, Q. H., Fatmous, M., Fang, H., Gurung, S., Vollenhoven, B., Salamonsen, L. A., & Greening, D. W. (2021). Proteomic profiling of human uterine extracellular vesicles reveal dynamic regulation of key players of embryo implantation and fertility during menstrual cycle. *Proteomics*, e2000211.

[98] Huang, D. W., Sherman, B. T., & Lempicki, R. A. (2009). Systematic and integrative analysis of large gene lists using DAVID bioinformatics resources. *Nature Protocols*, *4*(1), 44–57.

[99] Shi, W., Li, F., Li, S., Wang, J., Wang, Q., Yan, X., Zhang, Q., Chai, L., & Li, M. (2017). Increased DCLK1 correlates with the malignant status and poor outcome in malignant tumors: a meta-analysis. *Oncotarget*, *8*(59), 100545–100557.

[100] Bailey, J. M., Alsina, J., Rasheed, Z. A., McAllister, F. M., Fu, Y.-Y. Y., Plentz, R., Zhang, H., Pasricha, P. J., Bardeesy, N., Matsui, W., Maitra, A., & Leach, S. D. (2014). DCLK1 marks a morphologically distinct subpopulation of cells with stem cell properties in preinvasive pancreatic cancer. *Gastroenterology*, *146*(1), 245–256.

[101] Chandrakesan, Parthasarathy, May, R., Qu, D., Weygant, N., Taylor, V. E., Li, J. D., Ali, N., Sureban, S. M., Qante, M., Wang, T. C., Bronze, M. S., & Houchen, C. W. (2015). Dclk1+ small intestinal epithelial tuft cells display the hallmarks of quiescence and self-renewal. *Oncotarget*, *6*(31), 30876–30886.

[102] Vietri, M., Radulovic, M., & Stenmark, H. (2020). The many functions of ESCRTs. *Nature Reviews. Molecular Cell Biology*, *21*(1), 25–42.

[103] Colombo, M., Moita, C., van Niel, G., Kowal, J., Vigneron, J., Benaroch, P., Manel, N., Moita, L. F., Théry, C., & Raposo, G. (2013). Analysis of ESCRT functions in exosome biogenesis, composition and secretion highlights the heterogeneity of extracellular vesicles. *Journal of Cell Science*, *126*(24), 5553–5565.

[104] Wei, D., Zhan, W., Gao, Y., Huang, L., Gong, R., Wang, W., Zhang, R., Wu, Y., Gao, S., & Kang, T. (2021). RAB31 marks and controls an ESCRT-independent exosome pathway. *Cell Research*, *31*(2), 157–177.

[105] Jin, J., Xie, S., Sun, Q., Huang, Z., Chen, K., Guo, D., Rao, X., Deng, Y., Liu, Y., Li, S., Cui, W., Maibam, V. C., Wang, J., Zhuo, W., & Zhou, T. (2020). Upregulation of BCAM and its sense lncRNA BAN are associated with gastric cancer metastasis and poor prognosis. *Molecular Oncology*, *14*(4), 829–845.

[106] Nie, K., Shi, L., Wen, Y., Pan, J., Li, P., Zheng, Z., & Liu, F. (2020). Identification of hub genes correlated with the pathogenesis and prognosis of gastric cancer via bioinformatics methods. *Minerva Medica*, *111*(3), 213–225.

[107] Shen, H., Wang, L., Chen, Q., Xu, J., Zhang, J., Fang, L., Wang, J., & Fan, W. (2020). The prognostic value of COL3A1/FBN1/COL5A2/SPARC-mir-29a-3p-H19 associated ceRNA network in Gastric Cancer through bioinformatic exploration. *Journal of Cancer*, *11*(17), 4933–4946.

[108] Yuan, G., Zhang, B., Yang, S., Jin, L., Datta, A., Bae, S., Chen, X., & Datta, P. K. (2016). Novel role of STRAP in progression and metastasis of colorectal cancer through Wnt/β-catenin signaling.

Oncotarget, *7*(13), 16023–16037.

[109] Zhang, J., Huang, J. Y., Chen, Y. N., Yuan, F., Zhang, H., Yan, F. H., Wang, M. J., Wang, G., Su, M., Lu, G., Huang, Y., Dai, H., Ji, J., Zhang, J., Zhang, J. N., Jiang, Y. N., Chen, S. J., Zhu, Z. G., & Yu, Y. Y. (2015). Whole genome and transcriptome sequencing of matched primary and peritoneal metastatic gastric carcinoma. *Scientific Reports*, *5*(1), 13750.

[110] Jin, L., & Datta, P. K. (2014). Oncogenic STRAP functions as a novel negative regulator of E-cadherin and p21(Cip1) by modulating the transcription factor Sp1. *Cell Cycle (Georgetown, Tex.)*, *13*(24), 3909–3920.

[111] Lin, M.-T., Kuo, I.-H., Chang, C.-C., Chu, C.-Y., Chen, H.-Y., Lin, B.-R., Sureshbabu, M., Shih, H.-J., & Kuo, M.-L. (2016). Involvement of hypoxia-inducing factor-1α-dependent plasminogen activator inhibitor-1 up-regulation in Cyr61/CCN1-induced gastric cancer cell invasion. *The Journal of Biological Chemistry*, *291*(53), 27433.

[112] Slavin, T., Neuhausen, S. L., Rybak, C., Solomon, I., Nehoray, B., Blazer, K., Niell-Swiller, M., Adamson, A. W., Yuan, Y.-C., Yang, K., Sand, S., Castillo, D., Herzog, J., Wu, X., Tao, S., Chavez, T., Woo, Y., Chao, J., Mora, P., … Weitzel, J. (2017). Genetic Gastric Cancer Susceptibility in the International Clinical Cancer Genomics Community Research Network. *Cancer Genetics*, *216–217*, 111–119.

[113] Su, C., Wang, W., & Wang, C. (2018). IGF-1-induced MMP-11 expression promotes the proliferation and invasion of gastric cancer cells through the JAK1/STAT3 signaling pathway. *Oncology Letters*, *15*(5), 7000–7006.

[114] Wei, J., Yu, G., Shao, G., Sun, A., Chen, M., Yang, W., & Lin, Q. (2016). CYR61 (CCN1) is a metastatic biomarker of gastric cardia adenocarcinoma. *Oncotarget*, *7*(21), 31067–31078.

[115] Liu, Y., Ferguson, F. M., Li, L., Kuljanin, M., Mills, C. E., Subramanian, K., Harshbarger, W., Gondi, S., Wang, J., Sorger, P. K., Mancias, J. D., Gray, N. S., & Westover, K. D. (2020). Chemical Biology Toolkit for DCLK1 Reveals Connection to RNA Processing. *Cell Chemical Biology*, *27*(10), 1229-1240.e4.

[116] Koizumi, H., Fujioka, H., Togashi, K., Thompson, J., Yates, J. R., Gleeson, J. G., & Emoto, K. (2017). DCLK1 phosphorylates the microtubule-associated protein MAP7D1 to promote axon elongation in cortical neurons. *Developmental Neurobiology*, *77*(4), 493–510.

[117] Sheetz, M. P. (1996). Microtubule motor complexes moving membranous organelles. *Cell Structure and Function*, *21*(5), 369–373.

[118] Thul, P. J., Åkesson, L., Wiking, M., Mahdessian, D., Geladaki, A., Ait Blal, H., Alm, T., Asplund, A., Björk, L., Breckels, L. M., Bäckström, A., Danielsson, F., Fagerberg, L., Fall, J., Gatto, L., Gnann, C., Hober, S., Hjelmare, M., Johansson, F., … Lundberg, E. (2017). A subcellular map of the human proteome. *Science (New York, N.Y.)*, *356*(6340).

[119] Kumar, J., Yu, H., & Sheetz, M. P. (1995). Kinectin, an essential anchor for kinesin-driven vesicle motility. *Science (New York, N.Y.)*, *267*(5205), 1834–1837.

[120] Huang, J. D., Brady, S. T., Richards, B. W., Stenolen, D., Resau, J. H., Copeland, N. G., & Jenkins, N. A. (1999). Direct interaction of microtubule- and actin-based transport motors. *Nature*, *397*(6716), 267–270.

[121] Groth-Pedersen, L., Aits, S., Corcelle-Termeau, E., Petersen, N. H. T., Nylandsted, J., & Jäättelä, M. (2012). Identification of cytoskeleton-associated proteins essential for lysosomal stability and survival of human cancer cells. *PloS One*, *7*(10), e45381.

[122] Howard, T. L., Stauffer, D. R., Degnin, C. R., & Hollenberg, S. M. (2001). CHMP1 functions as a member of a newly defined family of vesicle trafficking proteins. *Journal of Cell Science*, *114*(Pt 13), 2395–2404.

[123] Harada, Y., Suzuki, T., Fukushige, T., Kizuka, Y., Yagi, H., Yamamoto, M., Kondo, K., Inoue, H., Kato, K., Taniguchi, N., Kanekura, T., Dohmae, N., & Maruyama, I. (2019). Generation of the heterogeneity of extracellular vesicles by membrane organization and sorting machineries. *Biochimica et Biophysica Acta. General Subjects*, *1863*(4), 681–691.

[124] Buljan, M., Ciuffa, R., van Drogen, A., Vichalkovski, A., Mehnert, M., Rosenberger, G., Lee, S., Varjosalo, M., Pernas, L. E., Spegg, V., Snijder, B., Aebersold, R., & Gstaiger, M. (2020). Kinase Interaction Network Expands Functional and Disease Roles of Human Kinases. *Molecular Cell*, *79*(3), 504-520.e9.

[125] Sugiyama, N., Imamura, H., & Ishihama, Y. (2019). Large-scale Discovery of Substrates of the Human Kinome. *Scientific Reports*, *9*(1), 10503.

[126] Cai, L., Holoweckyj, N., Schaller, M. D., & Bear, J. E. (2005). Phosphorylation of coronin 1B by protein kinase C regulates interaction with Arp2/3 and cell motility. *The Journal of Biological Chemistry*, *280*(36), 31913–31923.

[127] Hsu, W.-H., Yu, Y.-R., Hsu, S.-H., Yu, W.-C., Chu, Y.-H., Chen, Y.-J., Chen, C.-M., & You, L.-R. (2013). The Wilms' tumor suppressor Wt1 regulates Coronin 1B expression in the epicardium. *Experimental Cell Research*, *319*(10), 1365–1381.

[128] Williams, H. C., San Martín, A., Adamo, C. M., Seidel-Rogol, B., Pounkova, L., Datla, S. R., Lassègue, B., Bear, J. E., & Griendling, K. (2012). Role of coronin 1B in PDGF-induced migration of vascular smooth muscle cells. *Circulation Research*, *111*(1), 56–65.

[129] Werner, A.-C., Weckbach, L. T., Salvermoser, M., Pitter, B., Cao, J., Maier-Begandt, D., Forné, I., Schnittler, H.-J., Walzog, B., & Montanez, E. (2020). Coronin 1B Controls Endothelial Actin Dynamics at Cell-Cell Junctions and Is Required for Endothelial Network Assembly. *Frontiers in Cell and Developmental Biology*, *8*, 708.

[130] Cheng, X., Wang, X., Wu, Z., Tan, S., Zhu, T., & Ding, K. (2019). CORO1C expression is associated with poor survival rates in gastric cancer and promotes metastasis in vitro. *FEBS Open Bio*, *9*(6), 1097–1108.

[131] Ren, G., Tian, Q., An, Y., Feng, B., Lu, Y., Liang, J., Li, K., Shang, Y., Nie, Y., Wang, X., & Fan, D. (2012). Coronin 3 promotes gastric cancer metastasis via the up-regulation of MMP-9 and cathepsin K. *Molecular Cancer*, *11*, 67.

[132] Gao, W., Xu, J., Wang, F., Zhang, L., Peng, R., Shu, Y., Wu, J., Tang, Q., & Zhu, Y. (2015). Plasma membrane proteomic analysis of human Gastric Cancer tissues: revealing flotillin 1 as a marker for Gastric Cancer. *BMC Cancer*, *15*, 367.

[133] Pruksakorn, D., Klangjorhor, J., Lirdprapamongkol, K., Teeyakasem, P., Sungngam, P., Chaiyawat, P., Phanphaisarn, A., Settakorn, J., & Srisomsap, C. (2018). Oncogenic roles of serine-threonine kinase receptor-associated protein (STRAP) in osteosarcoma. *Cancer Chemotherapy and Pharmacology*, *82*(6), 1039–1047.

[134] Vukmirovic, M., Manojlovic, Z., & Stefanovic, B. (2013). Serine-threonine kinase receptor-associated protein (STRAP) regulates translation of type I collagen mRNAs. *Molecular and Cellular Biology*, *33*(19), 3893–3906.

[135] Brábek, J., Mierke, C. T., Rösel, D., Veselý, P., & Fabry, B. (2010). The role of the tissue microenvironment in the regulation of cancer cell motility and invasion. *Cell Communication and Signaling : CCS*, *8*, 22.

[136] Levental, K. R., Yu, H., Kass, L., Lakins, J. N., Egeblad, M., Erler, J. T., Fong, S. F. T., Csiszar, K., Giaccia, A., Weninger, W., Yamauchi, M., Gasser, D. L., & Weaver, V. M. (2009). Matrix crosslinking forces tumor progression by enhancing integrin signaling. *Cell*, *139*(5), 891–906.

[137] Lo, C. M., Wang, H. B., Dembo, M., & Wang, Y. L. (2000). Cell movement is guided by the rigidity of the substrate. *Biophysical Journal*, *79*(1), 144–152.

[138] Bartolini, A., Cardaci, S., Lamba, S., Oddo, D., Marchiò, C., Cassoni, P., Amoreo, C. A., Corti, G., Testori, A., Bussolino, F., Pasqualini, R., Arap, W., Corà, D., Di Nicolantonio, F., & Marchiò, S. (2016). BCAM and LAMA5 Mediate the Recognition between Tumor Cells and the Endothelium in the Metastatic Spreading of KRAS-Mutant Colorectal Cancer. *Clinical Cancer Research : An Official Journal of the American Association for Cancer Research*, *22*(19), 4923–4933.

[139] Jiang, Y., He, J., Guo, Y., Tao, H., Pu, F., & Li, Y. (2020). Identification of genes related to low-grade glioma progression and prognosis based on integrated transcriptome analysis. *Journal of Cellular Biochemistry*, *121*(5–6), 3099–3111.

[140] Yuan, L., Shu, B., Chen, L., Qian, K., Wang, Y., Qian, G., Zhu, Y., Cao, X., Xie, C., Xiao, Y., & Wang, X. (2017). Overexpression of COL3A1 confers a poor prognosis in human bladder cancer identified by co-expression analysis. *Oncotarget*, *8*(41), 70508–70520.

[141] Todorovic, V., Chen, C.-C., Hay, N., & Lau, L. F. (2005). The matrix protein CCN1 (CYR61) induces apoptosis in fibroblasts. *The Journal of Cell Biology*, *171*(3), 559–568.

[142] Juric, V., Chen, C.-C., & Lau, L. F. (2009). Fas-mediated apoptosis is regulated by the extracellular matrix protein CCN1 (CYR61) in vitro and in vivo. *Molecular and Cellular Biology*, *29*(12), 3266–3279.

[143] Chai, J., Norng, M., Modak, C., Reavis, K. M., Mouazzen, W., & Pham, J. (2010). CCN1 induces a reversible epithelial-mesenchymal transition in gastric epithelial cells. *Laboratory Investigation; a Journal of Technical Methods and Pathology*, *90*(8), 1140–1151.

[144] Bai, T., Chen, C.-C., & Lau, L. F. (2010). Matricellular Protein CCN1 Activates a Proinflammatory Genetic Program in Murine Macrophages. *The Journal of Immunology*, *184*(6), 3223–3232.

[145] Chen, C.-C., Young, J. L., Monzon, R. I., Chen, N., Todorović, V., & Lau, L. F. (2007). Cytotoxicity of TNFalpha is regulated by integrin-mediated matrix signaling. *The EMBO Journal*, *26*(5), 1257–1267.

Acknowledgements

This project was supported by a RFA Understanding Disease grant from La Trobe University to MB, a postgraduate research fellowship from La Trobe University to AC, a National Health and Medical Research Council of Australia (NHMRC) Senior Research Fellowship (1079257), Program Grant (1092788) and Investigator Grant (1183814) to ME. The authors also acknowledge support from the Operational Infrastructure Support Program of the Victorian Government, Australia to the Olivia Newton-John Cancer Research and Baker Heart and Diabetes Institute. This work was funded in part by NHMRC project grant (1139489 to DG), and Helen Amelia Hains Fellowship (to DG), a DF/HCC GI SPORE Developmental Research Project Award P50CA127003 (N.S.G.) and Hale Center for Pancreatic Research (N.S.G.).

Conflict of Interests:

F.M.F. and N.S.G. are inventors on a patent application related to the DCLK1 inhibitors described in this manuscript (WO/2018/075608). N.S.G. is a founder, science advisory board member (SAB) and equity holder in Gatekeeper, Syros, Petra, C4, B2S, Aduro, Jengu, and Soltego (board member). The Gray lab receives or has received research funding from Novartis, Takeda, Astellas, Taiho, Janssen, Kinogen, Voronoi, Her2llc, Deerfield and Sanofi.

Figure 1

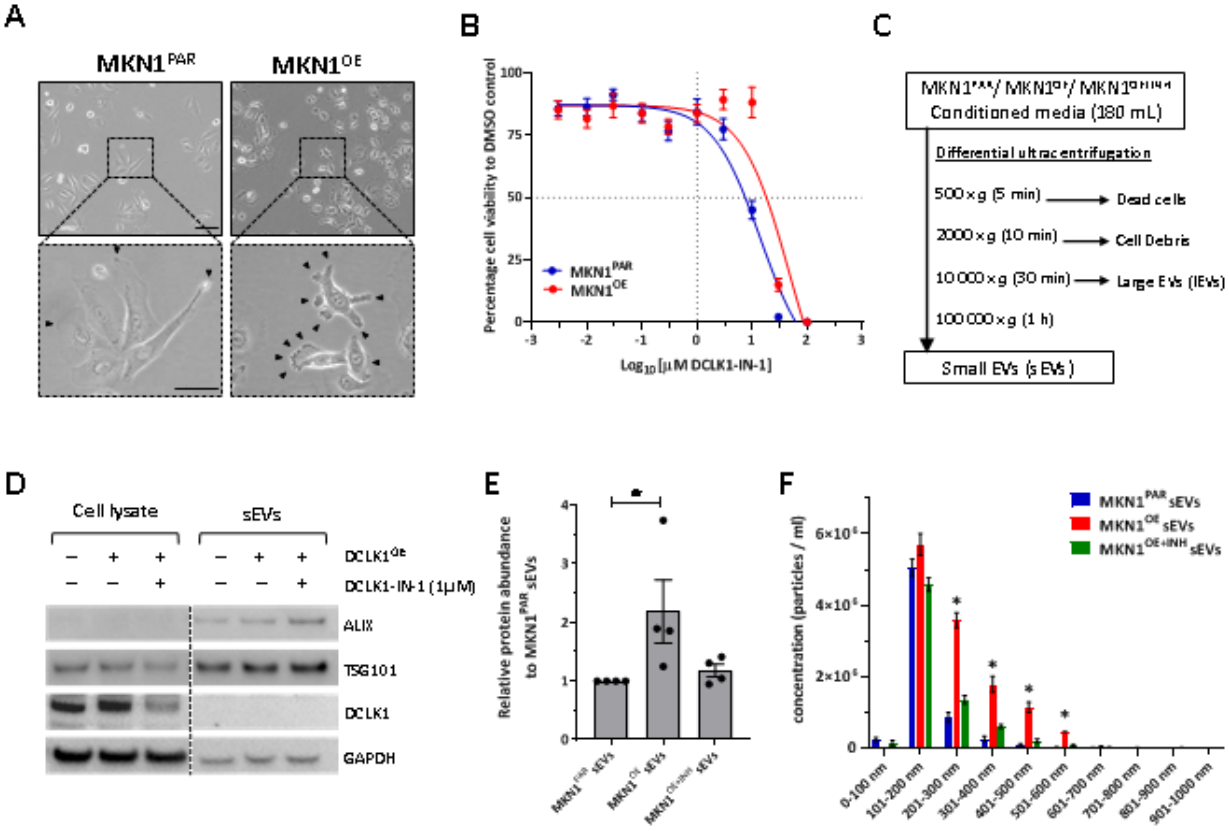

Figure 1. The effect of DCLK1 overexpression and inhibition on cell morphology and viability, and isolation and characterization of small extracellular vesicles from MKN1PAR, MKN1OE and MKN1OE+INH conditioned media. **A)** Morphological images of MKN1^{PAR} and MNK1^{OE} cells, scale bars = 20 µm, cell protrusions are indicated with arrowheads. **B)** DMSO normalized cell viability dose-response assay with DCLK1-IN-1 inhibitor. Data is represented as mean ± SEM of n = 4 technical replicates and are representative of n = 3 independent experiments, horizontal dotted line = IC_{50}, vertical dotted line = 1 µM of DCLK1-IN-1 inhibitor. **C)** Flow chart of the sEV isolation procedure by sequential differential centrifugation. **D)** Representative western blot for ALIX, TSG101, DCLK1, and GAPDH for full cell lysate and sEVs. **E)** Relative protein abundance of sEVs normalized to the MKN1^{PAR} subset of the same collection date. Data represented are average (n = 4) ± SEM (error bars), with unpaired Student's t-test, * p = 0.041. **F)** Histogram of Nanoparticle Tracking Analysis for particle concentration (particles/ml) and size distribution of sEVs of MKN1^{PAR} (blue), MKN1^{OE} (red) and MKN1^{OE+INH} (green), grouped per 100 nm. Data represent average of 5 replicate measurements ± SEM (error bars), * p < 0.001.

Figure 2

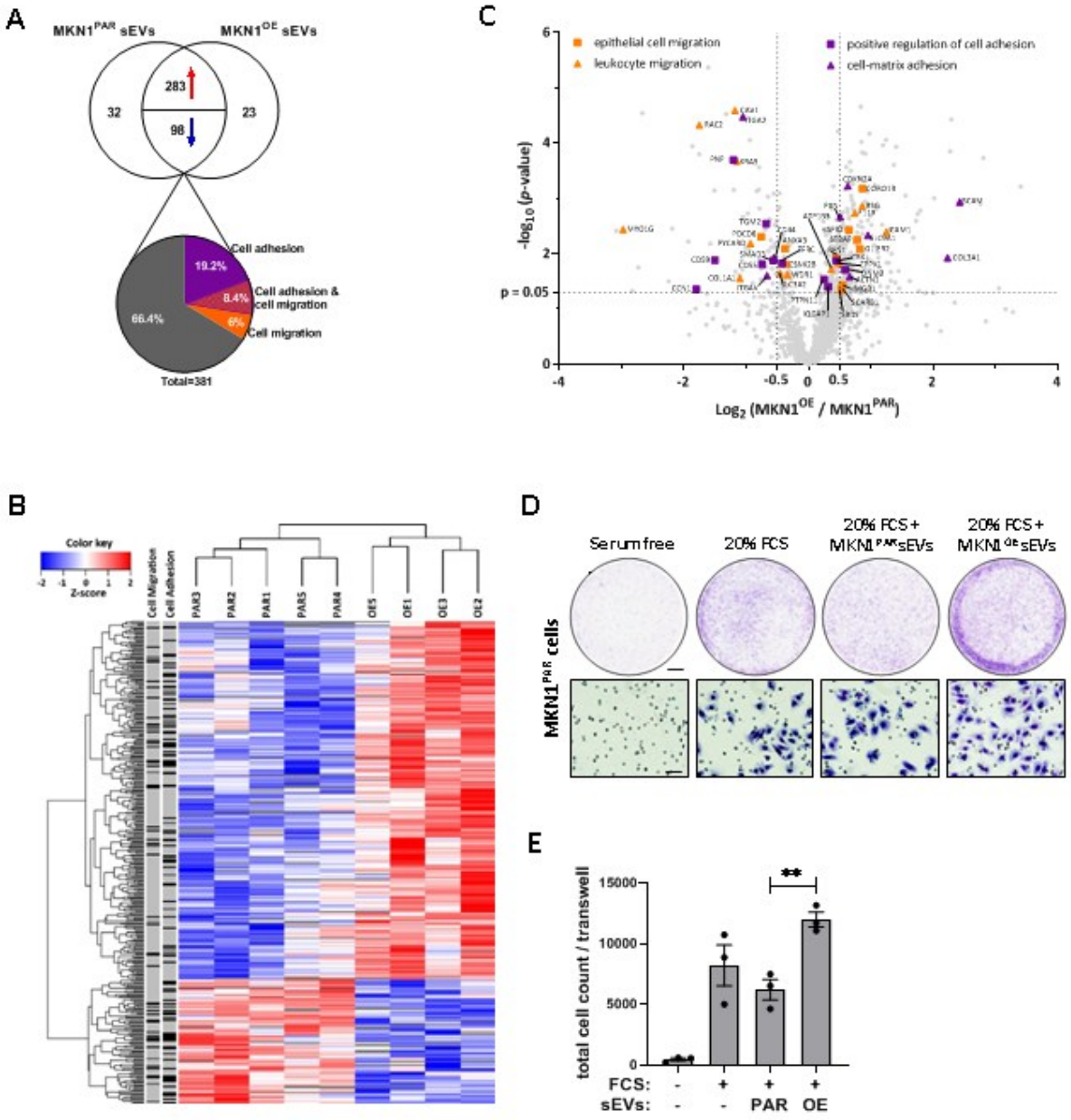

Figure 2. Overexpression of DCLK1 induces aberrant significant (p<0.05) differentially abundant proteins in sEVs isolated from MKN1. Proteins are present in >75% of replicates in at least one group. **A)** Overview of 55 unique and 381 significant differentially expressed proteins ($p < 0.05$) proteins in MKN1^{OE} sEVs in comparison to MKN1^{PAR} sEVs, showing the percentage of significant altered proteins associated with GO:0016477~cell migration, GO:0007155~cell adhesion, both or other GO-terms. **B)** Unsupervised clustering analysis of significantly differentially expressed proteins

($p<0.05$) for each replicate of MKN1^{PAR} (PAR) and MKN1^{OE} (OE) sEVs, values are z-scores of the LFQ intensities (missing values = grey), side columns link proteins are to GO:0016477~cell migration or GO:0007155~cell adhesion (black lines). **C)** Volcano plot showing differentially expressed proteins. The horizontal axis depicts the Log_2 fold change, the vertical axis represent the –Log(*p*-value, students t-test), with significance threshold at *p*-value = 0.05 (dashed line). Proteins are mapped to their GO-terms: epithelial cell (square) and leukocyte (triangle) migration (orange), positive regulation of cell adhesion (square, purple), or regulation of cell-matrix adhesion (triangle, purple) **D)** Representative images of the transwell migration membrane of MKN1^{PAR} cell with and without 20% FCS, and sEVs secreted by either MKN1^{PAR} or MKN1^{OE}. Scale bars: top row = 1 mm, bottom row = 50 µm. **E)** Nuclear cell count of Aperio^{TM} analysis of complete membrane of transwell migration assay in D (n = 3, error bars = SEM, *p*-value = 0.0053.

Figure 3

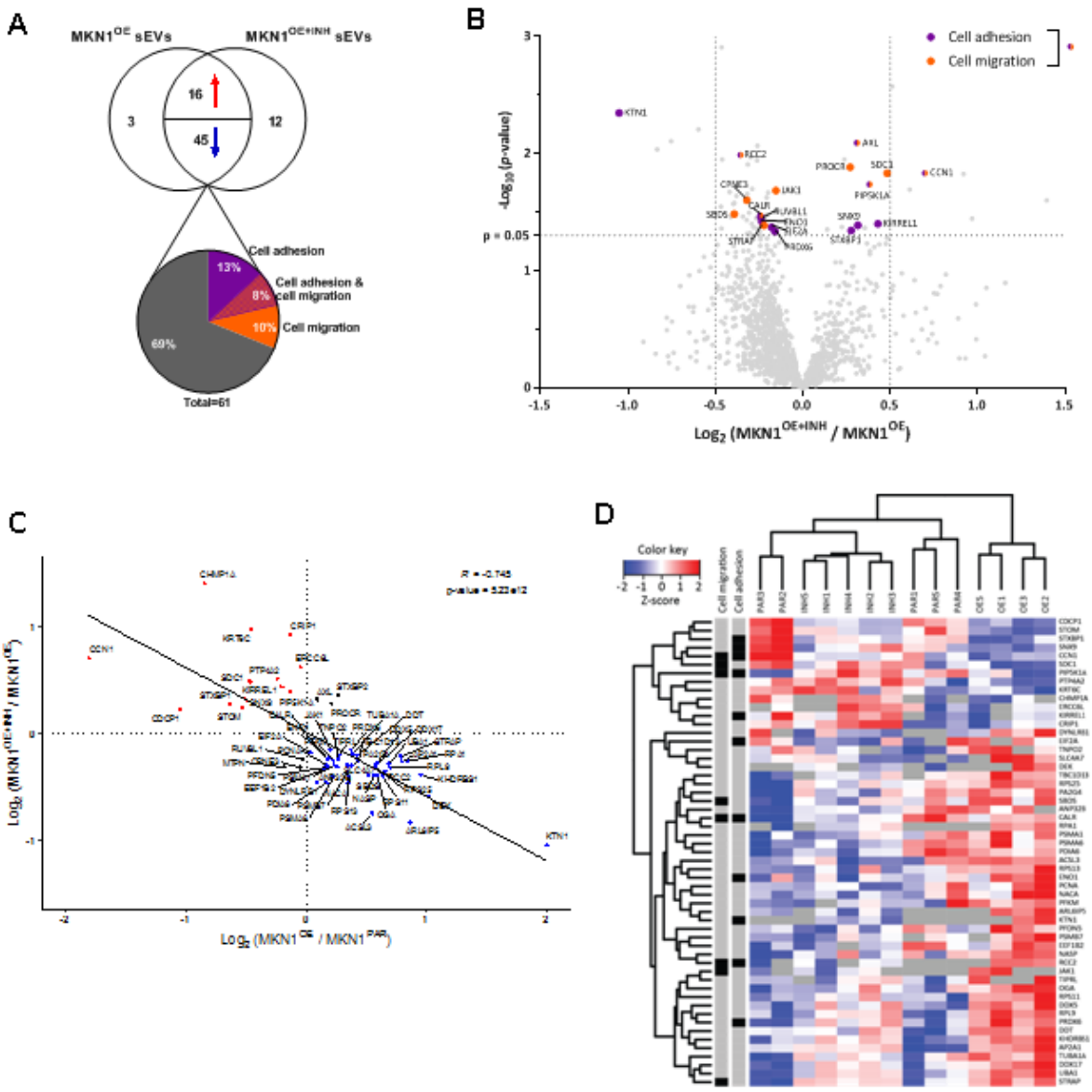

Figure 3. DCLK1-kinase dependent cargo selection for sEVs. DCLK1 overexpressing cells (MKN1^{OE}) treated with the small molecule inhibitor DCLK1-IN-IN (MKN1^{OE+INH}) resulted in significant differential expression of 61 proteins in sEVs. Proteins are present in >75% of replicates in at least one group. **A)** Overview of 15 unique and 61 significant differentially expressed proteins ($p < 0.05$) proteins in MKN1OE sEVs in comparison to MKN1PAR sEVs, showing the percentage of significant altered proteins associated with GO:0016477~cell migration (red), GO:0007155~cell adhesion (blue), both (checkered, red-blue), and other GO-terms (grey). **B)** Volcano plot showing differentially expressed

proteins; showing differential Log_2 FC of $MKN1^{OE+INH}$ *versus* $MKN1^{OE}$, the Y-axis shows the –Log(*p*-value, students t-test), with significance threshold at *p*-value 0.05 (dashed line). Proteins are mapped to their GO-terms: GO:0016477~cell migration (orange), GO:0007155~cell adhesion (purple) or both (red-blue halved circles). **C)** Correlation coefficient analysis of Log_2 fold change of $MKN1^{OE}$/$MKN1^{PAR}$ (x-axis) versus Log2 fold change of $MKN1^{OE+INH}$/$MKN1^{OE}$ (y-axis) of significantly differential proteins in response to DCLK1 inhibitor treatment. R-value represents Pearson correlation. **D)** Hierarchical clustering analysis (unsupervised clustering) of 55 kinase dependent proteins in sEVs from $MKN1^{PAR}$ (PAR), $MKN1^{OE}$ (OE) and $MKN1^{OE+INH}$ (INH); values are z-scores of LFQ intensities (missing values = grey), side columns link proteins are to GO:0016477~cell migration or GO:0007155~cell adhesion (black lines).

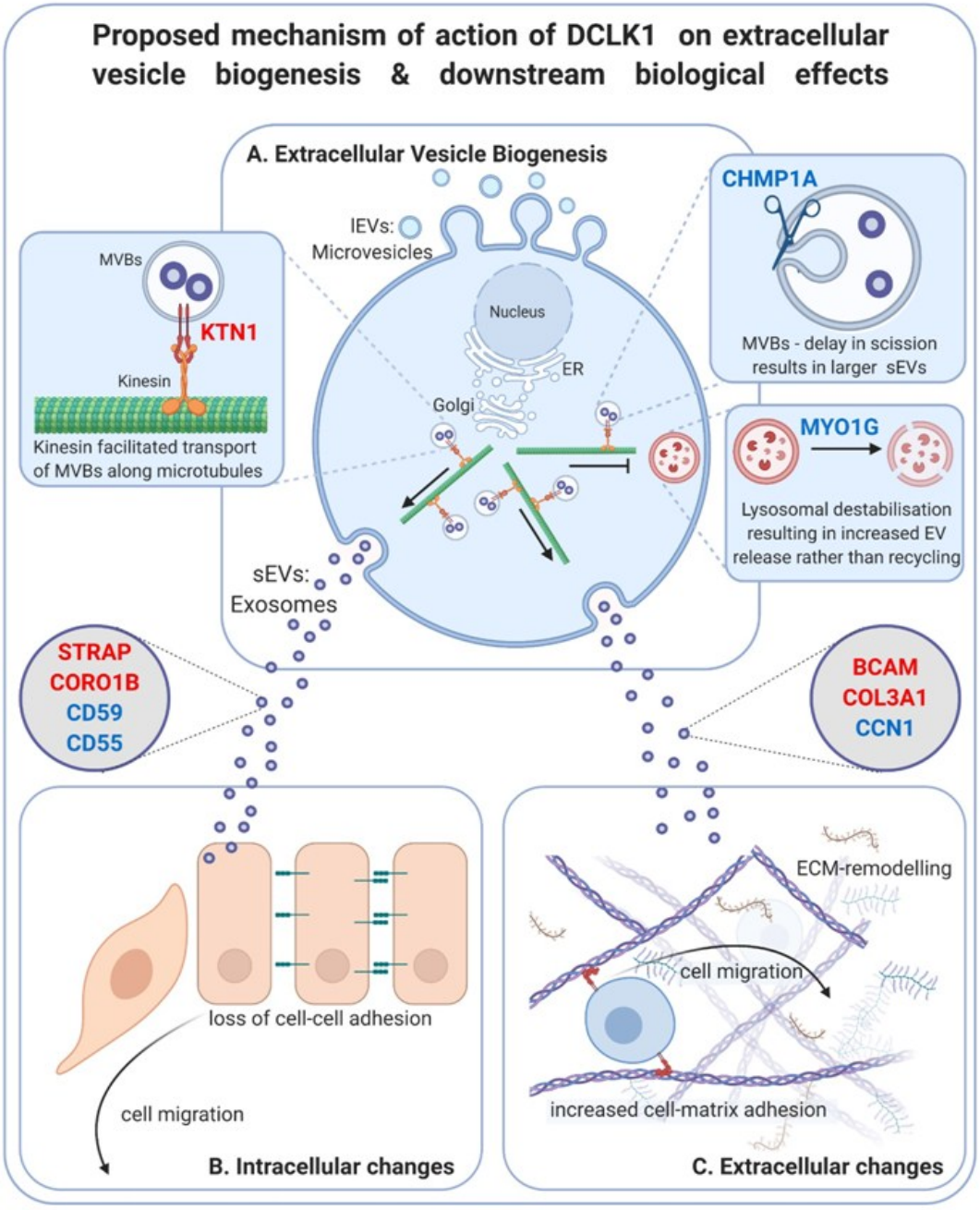

Figure 4. Schematic summary and proposed mechanism of action of DCLK1 on extracellular vesicle biogenesis & downstream biological effects. Throughout this figure sEV cargo proteins that are up-regulated are shown in red and down-regulated in cargo proteins are in blue. **A)** The effect of DCLK1 on extracellular vesicle biogenesis where KTN1 facilitates anchoring of multivesicular bodies (MVBs) to kinesins, therefore facilitating transport along microtubules. Lower CHMP1A levels might explain the larger vesicles found, CHMP1A is a regulator of vesicular scission. Lastly, down-regulation of MYO1G results in destabilization of lysosomes favoring the decision of sEVs to be released rather than recycled. **B)** These secreted sEVs can alter intracellular changes upon uptake and main al tered cargo proteins involving cell-cell adhesion and cell migration are: STRAP, CORO1B, CD59 and CD55. **C)** The effect of secreted sEVs on extracellular changes and ECM remodeling include altered cargo proteins BCAM, COL3A1 and CCN1 associated with cell-matrix adhesion and cell migration biological processes. Created with BioRender.com.